Li Chunlong (Orcid ID: 0000-0002-4693-2925)
Liu Ji-Hong (Orcid ID: 0000-0001-6686-1629)

SnRK2.4-mediated phosphorylation of ABF2 regulates *ARGININE DECARBOXYLASE* expression and putrescine accumulation under drought stress

Jie Song[1], Peipei Sun[2], Weina Kong[1], Zongzhou Xie[1], Chunlong Li[1], Ji-Hong Liu[1,*]

[1]Key Laboratory of Horticultural Plant Biology (MOE),
College of Horticulture and Forestry Sciences,
Huazhong Agricultural University,
Wuhan 430070,
China

[2]School of Horticulture,
Anhui Agricultural University,
Hefei 230036, China

Received: 8 August 2022

Accepted: 24 September 2022

***Corresponding author**

Ji-Hong Liu: liujihong@mail.hzau.edu.cn

ORCID

Jie Song: 0000-0001-5322-0179

Chunlong Li: 0000-0002-4693-2925

Ji-Hong Liu: 0000-0001-6686-1629

Summary

- Arginine decarboxylase (ADC)-mediated putrescine (Put) biosynthesis plays an important role in plant abiotic stress response. SnRK2s (SNF1-related protein kinases 2s) and ABFs, ABA-response element (ABRE) binding factors, are core components of ABA signaling pathway involved in drought stress response. We previously reported that *ADC* of *Poncirus trifoliata* (*PtrADC*) functions in drought tolerance. However, whether and how SnRK2 and ABF regulate *PtrADC* to modulate putrescine accumulation under drought stress remains largely unclear.
- Herein, we employed a set of physiological, biochemical, and molecular approaches to reveal that a protein complex composed of PtrSnRK2.4 and PtrABF2 modulates putrescine biosynthesis and drought tolerance by directly regulating *PtrADC*.
- *PtrABF2* was up-regulated by dehydration in an ABA-dependent manner. PtrABF2 activated *PtrADC* expression by directly and specifically binding to the ABRE core sequence within its promoter and positively regulated drought tolerance via modulating putrescine accumulation. PtrSnRK2.4 interacts with and phosphorylates PtrABF2 at Ser93. PtrSnRK2.4-mediated PtrABF2 phosphorylation is essential for the transcriptional regulation of *PtrADC*. Besides, PtrSnRK2.4 was shown to play a positive role in drought tolerance by facilitating the putrescine synthesis.
- Taken together, this study sheds new light on the regulatory module SnRK2.4-ABF2-*ADC* responsible for fine-tuning putrescine accumulation under drought stress, which advances our understanding on transcriptional regulation of putrescine synthesis.

Keywords: *Poncirus trifoliata*, drought stress, SnRK2, ABF, arginine decarboxylase, putrescine synthesis, protein phosphorylation.

Introduction

As sessile organisms, plants are frequently threatened by a variety of harsh environment conditions, among which drought is a major detrimental factor that restricts plant growth and development and causes a significant loss of crop productivity throughout the world (Zandalinas *et al*., 2018; Chen *et al*., 2021). Breeding drought-tolerant crops by manipulating genes conferring drought tolerance is a promising and attractive approach to address the challenges rendered by drought (Furihata *et al*., 2006). In this regard, it is imperative and pressing to understand the molecular mechanisms by which plants respond and adapt to the drought stress so as to unravel the pertinent genes or gene cascades that play crucial roles in modulation of drought tolerance.

It is well known that plants have evolved delicate and complicated defensive mechanisms that enable them to avoid and tolerate the abiotic stress in a timely manner (Zhang *et al*., 2022b; Zandalinas and Mittler, 2022). To withstand the drought stress plants may undergo a range of physiological, biochemical, and metabolic changes, among which accumulation of various secondary metabolites has been suggested to function directly in coping with the imposing stressor through different protective processes, such as stress-derived damage repair, cellular homeostasis maintenance and growth adjustment (Hu *et al*., 2016; Gupta *et al*., 2020; Zhao *et al*., 2020). It is worth mentioning that such changes are largely attributed to reprogramming a wide spectrum of genes associated with related metabolic pathways.

A range of metabolites, including polyamines (PAs), have been reported to accumulate and function to minimize the adverse effects of drought stress imposed on plants (Shi *et al*., 2014; Liu *et al*., 2015; Wang *et al*., 2019; Zandalinas *et al*., 2022). PAs, primarily diamine putrescine (Put), triamine spermidine (Spd), and tetramine spermine (Spm), are low-molecular-weight aliphatic nitrogenous compounds that are ubiquitously present in higher plants. Putrescine is an important intermediate connecting PA synthesis with other metabolic processes and acts as the substrate for Spd and Spm, suggesting its crucial role in orchestration of PA synthesis. In higher plants, putrescine can be produced from ornithine or arginine, catalyzed by ornithine decarboxylase (ODC; EC 4.1.1.17) and arginine decarboxylase (ADC; EC 4.1.1.19), respectively (Paschalidis & Roubelakis-Angelakis, 2005; Liu *et al*., 2006). So far, numerous studies have shown that putrescine

accumulation is a common phenomenon observed in plants subjected to abiotic stresses, including drought. Consistent with the elevation of putrescine content, *ADC* transcript levels have been shown to be drastically elevated in most, if not all, examined plants treated by drought, implying that the ADC pathway plays a dominant role in modulation of putrescine synthesis under abiotic stresses (Alcázar *et al*., 2010b; Liu *et al*., 2015; Tsaniklidis *et al*., 2020).

Stress-responsive genes are categorized into two major groups, functional and regulatory, based on the precise role of the genes and their products in stress tolerance (Liu *et al*., 2014; Song *et al*., 2016). The functional genes are fine-tuned by upstream regulators, including transcription factors and proteins responsible for protein modification at posttranscriptional, translational, and posttranslational levels (Reyes *et al*., 2010; Lyzenga *et al*., 2012; Song *et al*., 2021; Zhang *et al*., 2022b). These components constitute the major interconnecting module responsible for orchestrating stress-triggered cell signaling, ranging from stress sensing, signal amplification and transduction to stress response. Therefore, it is of tremendous value to decipher the signaling module associated with the regulation of a given metabolic pathway. As such, enormous progresses have been made to understand the regulatory modules pertinent to the secondary metabolites implicated in different physiological or biological processes. For example, numerous TFs that act as either positive or negative regulators for metabolites synthesis have been identified in various plant species, which greatly promoted our understanding of the regulatory signaling network implicated in abiotic stress due to metabolites accumulation (Wang *et al*., 2020; Li *et al*., 2021; Zhao *et al*., 2021; Ge *et al*., 2022). So far, several TFs, including WRKY70, NAC72, CBF1, and ABF4 have been revealed to possibly regulate the *ADC* gene expression and putrescine accumulation in response to drought or cold stresses (Gong *et al*., 2015; Zhang *et al*., 2015; Wu *et al*., 2016; Song *et al*., 2022). However, it needs to be pointed out that the regulatory cascade responsible for *ADC* upregulation and putrescine accumulation in response to drought conditions remains far from being understood. No proteins that act as interacting partners and modifiers of the TFs regulating *ADC* expression have been clarified yet, which impedes the illustration of in-depth molecular mechanisms underlying the *ADC*-mediated putrescine accumulation under stressful cues.

Abiotic stress signals are relayed and transduced by various second messengers, including the plant hormones. Abscisic acid (ABA) is a well-characterized phytohormone that plays a critical role in orchestrating a spectrum of specific signal transduction, contributing to regulation of downstream genes responsible for combating the drought stress (Zhu *et al*., 2002; Hyunhee *et al*., 2019; Zhang *et al*., 2022b). During the last two decades, enormous studies have been devoted to identifying the core components necessary for the ABA signaling network and explicitly deciphering their mode of action on regulating the expression of ABA-responsive genes. In brief, ABA is perceived by the ABA receptors (Pyrabactin Resistance1/PYR1-like/Regulatory Components of ABA Receptors, PYR/PYL/RCARs), and promotes the interaction between PYR/PYL/RCARs and clade A phosphatase type 2C (PP2C). This will inhibit the phosphatase activity of PP2C to release the SnRK2s, which in turn phosphorylate and activate downstream TFs (Ma *et al*., 2009; Park *et al*., 2009; Soon *et al*., 2012; Zhao *et al*., 2018). The basic leucine zipper (bZIP) family transcription factors, such as ABFs (ABA-response element binding factors), are the major targets of SnRK2 in the ABA core signaling pathway (Cutler *et al*., 2010; Fujita *et al*., 2013; Saruhashi *et al*., 2015; Yoshida *et al*., 2015). For example, in a very recent study two bZIP TFs, including bZIP29 and Opaque2, were phosphorylated by SnRK2.2 to transactivate downstream target genes for endosperm filling in maize (Yang *et al*., 2022). In addition, either SnRK2s or ABFs have been separately shown to act as the pivotal regulators of various physiological and biological processes, such as root growth (Liu *et al*., 2021), stomatal development (Ding *et al*., 2020), sugar metabolism (Ma *et al*., 2017b), flower senescence (Liu *et al*., 2017), abiotic stress response (Chen *et al*., 2020; Takahashi *et al*., 2020; Li *et al*., 2021), among others. As increasing evidence showed that activation of ABFs requires the SnRK2s-mediated phosphorylation (Kobayashi *et al*., 2005; Wang *et al*., 2012; Umezawa *et al*., 2013; Wang *et al*., 2019), it is reasonable to assume that the SnRK2s and ABFs in various combination might function in synergy to play crucial roles in regulation of the plant development and responses to environmental stresses. However, it remains elusive whether and how a SnRK2-ABF complex regulates the *ADC* expression and putrescine accumulation in response to drought stress.

Trifoliate orange (*Poncirus trifoliata*), a plant closely related to citrus, is widely

used as rootstock for citrus industry. However, trifoliate orange is not drought-tolerant, thus limiting plant performance of citrus trees in the regions with water shortage or limited irrigation facilities. We have previously characterized the function and physiological relevance of *PtrADC* (*Poncirus trifoliata ADC*, formerly named *PtADC*) in drought tolerance (Wang et al., 2011). In addition, by performing yeast one-hybrid cDNA library screening using *PtrADC* promoter (pADC), we unraveled a candidate TF annotated as ABF2, which was designated as PtrABF2 (*Poncirus trifoliata* ABF2) hereafter. We thus hypothesize that PtrABF2 may act as a critical regulator of drought tolerance in trifoliate orange by modulation of putrescine content through regulating *PtrADC*. In the present study, we first verified the interaction between PtrABF2 and pADC, and functionally characterized the role of PtrABF2 in modulation of *PtrADC* expression and putrescine for imparting drought tolerance. We further characterized that *PtrSnRK2.4*, the PtrSnRK2 family member exhibiting the greatest induction by ABA, interacted with and phosphorylated PtrABF2 at Ser93. PtrSnRK2.4-mediated phosphorylation was then shown to be critical for the interaction and transactivation of PtrABF2 with pADC. Finally, we confirmed that *PtrSnRK2.4* played a positive role in drought tolerance by modulation of *PtrADC*-mediated putrescine synthesis. Taken together, we illustrated the molecular mechanisms by which *PtrSnRK2.4* controlled drought tolerance and putrescine synthesis via phosphorylation of PtrABF2, leading to transcriptional regulation of *PtrADC*. The established regulation module composed of SnRK2.4-ABF2-*ADC* will advance our understanding on the *ADC* up-regulation and putrescine accumulation in response to drought stress. Moreover, the genes identified in this study can be applied for genetic manipulation in breeding efforts to produce drought-tolerant fruit crops.

Materials and Methods

Plant materials and growth conditions

Trifoliate orange seeds (*Poncirus trifoliata* L. Raf.) collected from a germplasm repository at Huazhong Agricultural University were grown in soil pots at 25 °C under long days (16-h light/8-h dark). For dehydration treatment, 3-month-old plants were incubated for 3 d in water or 100 μM fluridone (Ehrenstorfer, Augsburg, Germany) solution, and the leaves were then detached and desiccated on filter papers at ambient temperature. For ABA and

salt treatments, the plants were incubated in solutions containing either 100 μM ABA or 250 mM NaCl. For cold treatment, trifoliate orange plants grown at ambient temperature were shifted to low temperature (4 °C) growth incubator. Leaves were harvested at the designated time points, rapidly frozen in liquid nitrogen, and stored at -80 °C for further analysis.

RNA extraction and quantitative real-time RT-PCR analysis

For expression analysis, total RNA was extracted using a commercial RNA extraction kit (RN33; Aidlab Biotech Co. Ltd, Beijing, China), and then reversely transcribed into cDNA (complementary DNA) using RevertAid^{TM} First Strand cDNA Synthesis Kit (Thermo Fischer Scientific, Waltham, MA, USA) with an oligo(dT) primer according to the manufacturer's instructions. Quantitative real-time PCR (qPCR) was performed using the AceQ SYBR Green Master Mix (Vazyme, Nanjing, China) on an ABI7500 system (Applied Biosystems, Foster City, CA, USA). The amplification reactions were carried out at 95 °C for 5 min, followed by 40 cycles of 95 °C for 10 s, 58 °C for 30 s, and 95 °C for 15 s, in a 10 μL reaction mixture composed of 5 μL 2× SYBR Green PCR master mix, 0.4 μL primers, and 200 ng cDNA. Three replicates were performed for each sample. *Actin* was used as internal reference genes in all experiments to normalize expression levels of examined the genes according to the $2^{(-\Delta\Delta CT)}$ algorithm (Livak & Schmittgen, 2001). Sequences of relevant primers used in this study are listed in Table S1.

Plasmid construction and transformation

The coding sequences (CDS) of *PtrSnRK2.4* and *PtrABF2* were amplified from a full-length cDNA (complementary DNA) of trifoliate orange, and inserted into pBI121, driven by the CaMV *35S* promoter, to generate overexpression vectors. To construct the virus-induced gene silencing (VIGS) constructs, cDNA fragments of *PtrSnRK2.4* (474 bp) and *PtrABF2* (510 bp) were amplified and integrated into the tobacco rattle virus-based vector 2 plasmid (pTRV2). All fusion constructs were introduced into *Agrobacterium tumefaciens* strain GV3101 by heat shock. *Agrobacterium* -mediated transformation of lemon shoot segments was done following earlier report (Fu *et al.*, 2011), whereas the VIGS constructs were employed to transfect 1-month-old trifoliate orange seedlings as

previously described (Dai *et al*., 2018). The positive transgenic plants were verified by genomic PCR using two pairs of specific primers, while transcript levels of the transgenes were confirmed by qPCR.

Subcellular localization analysis

The coding sequences (CDS) of *PtrSnRK2.4* and *PtrABF2* without the stop codons were inserted into the 101LYFP vector at the *Xba* I and *Bam*H I restriction sites between the CaMV *35S* promoter and the YFP (yellow fluorescent protein) CDS. The vectors were separately introduced into *A. tumefaciens* GV3101 strain. The fusion vectors and the YFP control, along with the plasmids expressing a nuclear marker (35S: VirD2NLS−mCherry, Kumar & Kirti, 2010) or membrane marker (35S: CBL1n-OFP, Meng *et al*., 2020), were transiently expressed in leaves of tobacco (*Nicotiana benthamiana*) via *Agrobacterium*-mediated infiltration. After incubation for 48 h at 24 °C under light conditions, the fluorescence signals were detected using a confocal laser scanning microscope (Leica TCS-SP8, Wetzlar, Germany).

Transcriptional activation assay

The full-length CDS of *PtrABF2* was inserted into the pGBKT7 vector (Clontech), and the recombinant plasmid was transferred to yeast strain AH109 (Takara, Japan). The yeast cells were serially diluted and cultured on SD/-Trp and SD/-Trp/-His/-Ade media with 40 μg mL^{-1} 5-bromo-4-chloro-3-indolyl-a-D-galactopyranoside (X-α-gal, Sigma-Aldrich, St Louis, MO, USA). The pGBKT7-53 + pGADT7-T vector and pGBKT7 were used as positive and negative controls, respectively. Transcriptional activation activity was detected based on the growth of yeast cells and the activation of the HIS4 reporter.

Yeast one-hybrid (Y1H) assay

For Y1H assay, a 412-bp fragment (P1) of pADC containing the canonical ABRE element (ACGTGG) was amplified by genomic PCR. In addition, another fragment (412 bp) harboring the mutated ABRE sequence (TTTGTG) was synthesized based on P1 sequence to generate mP1. Both P1 and mP1 were inserted into the pAbAi vector at the *Kpn* I and *Xho* I sites to generate two baits. The full-length open reading frame (ORF) of *PtrABF2*

was amplified and fused to the pGADT7 vector to obtain a prey vector. The prey vector was transformed into the bait-harboring reporter strain using the Matchmaker Y1H library Screening System (Clontech, Mountain View, CA, USA) following the manufacturer's protocol. The yeast cells, along with the positive (pGAD-p53+p53-AbAi) and negative (pGADT7+P1-AbAi) controls, in two dilutions, were streaked on SD/-Ura/-Leu medium added with or without 200 ng mL^{-1} Aureobasidin A (AbA, Coolaber, Beijing, China) and kept at 30 °C for 3 d.

Transient dual luciferase (LUC) assays

For dual LUC assays, the effector constructs were generated by cloning the full-length CDS of *PtrABF2* and *PtrSnRK2.4* into pGreenII 62-SK vector (Hellens *et al.*, 2005) under the control of CaMV *35S* promoter. In addition, site-directed mutagenesis was conducted to produce $PtrABF2^{S93A}$, in which Ser (Serine) 93 of PtrABF2 was mutated into Ala (Alanine). To this end, the cDNA was PCR amplified with the proofreading DNA polymerase and corresponding primers containing the pertinent mutations. P1 and mP1 were inserted into pGreenII 0800-LUC to generate two reporter constructs, in which *REN* (*Renilla luciferase*) gene in the reporter plasmid, under the control of CaMV *35S* promoter, was used as an internal control. Bacterial solutions of effector and reporters were prepared and transiently infiltrated in the leaves of 4-week-old tobacco (*N. benthamiana*) plants, followed by measurement of LUC and REN activities using the Dual-LUC Reporter Assay System kit (Promega, Madison, WI, USA) on an Infinite 200 PRO microplate reader (Tecan, Mannedorf, Switzerland). The promoter activity was expressed as LUC/REN ratio. In addition, D-luciferin was applied on the adaxial side of the leaves before observation of the LUC fluorescence using Night SHADE LB985 chemiluminescent imaging system (Berthold, Germany).

Electrophoretic mobility shift assay (EMSA)

The full-length CDS of *PtrSnRK2.4* was cloned into the pHGWA vector with a His tag, while *PtrABF2* and $PtrABF2^{S93A}$ CDS were cloned into the pGEX6P-1 vector containing a GST tag. The vectors were transformed in *Escherichia coli* strain BL21 (DE3). The recombinant proteins were induced at 37 °C, and purified in its native form using either

glutathione agarose resin (Beyotime, China) for GST-PtrABF2 and GST-PtrABF2^{S93A} or Ni-NTA agarose (Qiagen, Hilden, Germany) for His-PtrSnRK2.4 according to the manufacturer's instructions. Oligonucleotide probes (40 bp) containing either wild-type or mutated ABRE were synthesized based on sequence of P1/mP1, and labeled with biotin at the 5' terminals by Tsingke Biotechnology (Beijing, China), whereas unlabeled wild-type probe was used as a competitor. EMSA was carried out using a Chemiluminescent EMSA Kit (Pierce Biotechnology, IL, USA) according to the manufacturer's protocols. Visualization was conducted using the Chemiluminescence Nuclei Acid Detection Module (Thermo Fisher Scientific).

Chromatin immunoprecipitation (ChIP)-qPCR assay

The CDS of *PtrABF2* was cloned in frame to the 5' end of the GFP gene in pGWB405, generating 35S::PtrABF2-GFP. The fusion construct was introduced into *A. tumefaciens*, which was then used to transform sweet orange callus. Expression of the transgene in the callus was confirmed by western blotting using anti-GFP antibody (Abbkine, a02020, Wuhan, China) and HRP goat anti-mouse IgG (H+L) antibody (ABclonal, aS003). ChIP assays were performed as previously described (Ming *et al.*, 2020). In brief, the transgenic and untransformed calli were crosslinked for 20 min by immersing in 1% formaldehyde solution, followed by random shearing of the genomic DNA through sonication. The extracted protein/chromatin complexes were collected with anti-GFP mAb-magnetic agarose bead (MBL, Nagoya, Japan). The resulting DNA was used for quantitative PCR analysis using specific primers designed according to the sequence of pADC. Actin was used as a control for calculating the enrichment of PtrABF2 on the DNA fragments, as has been reported by Chen *et al.* (2018).

Yeast two-hybrid (Y2H) assay

The constructs for Y2H assays were generated by cloning the full-length CDS of *PtrSnRK2.4* into pGADT7 vector containing the activation domain, while the full-length and truncated halves (either N- or C-terminal) of *PtrABF2* CDS were individually cloned into pGBKT7 vector containing the binding domain. The constructs were then co-transformed into the yeast (*Saccharomyces cerevisiae*) strain Y2HGold following the

Matchmaker™ Gold Yeast Two-Hybrid System protocol (TaKaRa, Japan). The protein-protein interaction was assessed by monitoring the growth and α-galactosidase activity of the co-transformed yeast cells, after serial dilutions, on SD/-Trp/-Leu and SD/-Trp/-Leu/-His/-Ade medium added with 40 μg mL^{-1} X-α-gal (Sigma-Aldrich, St Louis, MO, USA) and 100 ng mL^{-1} AbA (Coolaber, Beijing, China). The empty pGBKT7 vector was co-transformed in parallel as a negative control.

Bimolecular fluorescence complementation (BiFC) assays

For BiFC assay, the full-length CDS of *PtrSnRK2.4* was cloned into the L101YCE vector containing the C-terminal region of yellow YFP to obtain SnRK2.4-cYFP, while the full-length CDS of *PtrABF2* was fused to the L101YNE vector containing the N-terminus of YFP to obtain ABF2-nYFP. The vectors AtZIP63-cYFP and AtZIP63-nYFP were used as positive control, whereas the empty vectors L101YCE (cYFP) and L101YNE (nYFP) were used as negative control. The constructs were introduced into *A. tumefaciens* strain GV3101, and the bacterial suspensions were mixed and infiltrated into the abaxial side of leaves of 28-d-old *N. benthamiana* plants, followed by observation of YFP fluorescence under the confocal laser scanning microscope (TCS-SP8, Leica Wetzlar, Germany).

Luciferase complementation imaging (LCI) assay

For LCI assays, the full-length CDS of *PtrSnRK2.4* and *PtrABF2* were cloned into the JW771 (nLUC) and JW772 (cLUC) vectors (Gou *et al*., 2011), generating nLUC-PtrSnRK2.4 and cLUC-PtrABF2. The recombinant plasmids, along with the empty vector (nLUC and cLUC), were introduced into *Agrobacterium tumefaciens* strain GV3101 harboring the helper plasmids pSoup and P19. The bacterial suspensions harboring respective constructs were mixed and then used to infiltrate leaves of *N. benthamiana*, followed by visualization of LUC fluorescence.

In vitro Pull-down assays

The GST pull-down assays were performed using two fusion proteins GST-PtrABF2 and His-PtrSnRK2.4, as has been previously described (Ma *et al*., 2017a). Briefly, the recombinant proteins, were induced in *E. coli* BL21 (DE3) cells as mentioned above for

EMSA assay. The proteins were mixed and incubated with glutathione-agarose resin (Beyotime, China) for 4 h at 4 °C with gentle rotation according to the manufacturer's protocol. The samples were washed at least three times in the lysis buffer (10 mM Tris-HCl at pH 7.5, 100 mM NaCl, 1 mM β-mercaptoethanol, 1 mM EDTA, 10% glycerol (v/v), with 0.5% Triton X-100 (v/v)) to remove unbound proteins, and the remaining proteins were eluted in the elution buffer (lysis buffer + 10 mM glutathione, pH 8.0). The eluted proteins were then subjected to immunodetection with the anti-GST or anti-His antibodies (TransGen Biotech, Beijing).

Phosphorylation assays and liquid chromatography-mass spectrometry (LC-MS/MS)

In vitro phosphorylation assay using recombinant fusions, including GST-PtrABF2, GST-ABF2^{S93A} and His-PtrSnRK2.4 (Zhou *et al.*, 2018). For *in planta* phosphorylation, the full-length *PtrSnRK2.4* cDNA was cloned in pGWB414 to get 35S:PtrSnRK2.4-HA, while *PtrABF2* or *PtrABF2^{S93A}* cDNA was cloned into pGWB405 to generate 35S:PtrABF2-GFP or 35S:PtrABF2^{S93A}-GFP, respectively. PtrSnRK2.4-HA was co-expressed with either PtrABF2-GFP or PtrABF2^{S93A}-GFP in *N. benthamiana* leaves, which were subjected to protein extraction and immunoprecipitation using anti-GFP agarose beads (MBL, Nagoya, Japan) according to Hu *et al.* (2021). The immunoprecipitated proteins were separated in the SDS-PAGE (sodium dodecyl sulfate-polyacrylamide gel electrophoresis). The *in vitro* and *in vivo* phosphorylation of recombinant proteins was determined by immunoblotting with antibody anti-pSer/pThr (ECM Biosciences, PM3801). The protein inputs were detected by immunoblotting with anti-His or anti-GST antibodies (TransGen Biotech, Beijing) for *in vitro* assay or with anti-HA or anti-GFP antibodies (Abbkine, Wuhan, China) for *in planta* assay.

Phosphorylation sites were determined by performing LC-MS/MS. To this end, the purified GST-PtrABF2 and His-PtrSnRK2.4 proteins were incubated for 30 min at 30 °C in the abovementioned phosphorylation reaction buffer prior to separation in separation in SDS-PAGE. Then, the gel band containing phosphopeptides was analyzed with Thermo-Scientific, Q-exactive HF-X (Bioprofile, Shanghai, China).

Drought tolerance assays of transgenic plants

For the drought tolerance assays, the wild type (WT) lemon and transgenic plants, the TRV control and VIGS line, without or with pretreated of 10 mM putrescine for 3 d, were deprived of watering for 25 d at ambient temperature with a 16-h-light/8-h-dark photoperiod (with a white light intensity of 80 μM photons m^{-2} s^{-1}). The plants were then rewatered and grew for another 3 d. Growth performance and fluorescence imaging of the plants were monitored before and after the drought treatment, while the leaves were sampled for further analyses.

Physiological measurements and histochemical staining

Electrolyte leakage (EL) was measured by investigating relative conductance as previously described (Dai *et al.* 2018). Briefly, leaves were placed in Eppendorf tubes filled with 20 ml of ddH_2O, using tubes containing same volume of water as control. The tubes were shaken on a shaker (Qilinbeier, China) for 1 h (20 rpm) at room temperature, and then the initial conductivity values of the sample (C1) and the control (CK1) were measured using a conductivity meter (DSS-307, SPSIC, China). The tubes were then boiled for 10 min and cooled at room temperature before measuring a second conductivity (C2 and CK2 for sample and control, respectively). EL of the samples was calculated as C(%) = (C1−CK1)/(C2−CK2)×100. MDA content, anti- $O_2^{\cdot-}$ activity (which is negatively proportional to $O_2^{\cdot-}$ level), and H_2O_2 levels were determined using analytical kits (Nanjing Jiancheng Bioengineering Institute, Nanjing, China) according to the manufacturer's instructions. Total protein was colorimetrically measured with UV-vis spectrophotometer (UV-2600, Shimadzu, Japan) using Coomassie Brilliant Blue G-250 staining (Bradford. 1976). *In situ* accumulation of H_2O_2 and $O_2^{\cdot-}$ was assessed by histochemical staining with 3, 3'-diaminobenzidine (DAB) and nitro blue tetrazolium (NBT), respectively (Huang *et al.*, 2013). Chlorophyll fluorescence imaging was recorded with an IMAGINGPAM chlorophyll fluorimeter, and Fv/Fm ratios were calculated using Imaging WinGigE software (Walz, Germany).

Quantification of putrescine levels and ADC activity

Putrescine was extracted and measured as described previously (Liu *et al.*, 2006; Fu *et al.*, 2011; Gong *et al.*, 2015; Wu *et al.*, 2016). Briefly, about 0.1 g of sample was extracted in

1 ml of 5% cold perchloric acid (PCA) containing dithiothreitol (0.5 g L^{-1}). The homogenate was centrifuged at 500 ×*g* for 5 min, and the resulting upper phase was collected and vacuum-dried in a concentrator (SCANVAC, Vassingerod, Denmark). After dissolution in PCA, putrescine level, expressed as a nmol g^{-1} fresh weight (FW), in the suspension were analyzed on an HPLC system (Agilent, Santa Clara, CA, USA), using 1,6-hexanediamine as the internal standard. ADC activity was analyzed by the enzyme-linked immunosorbent assay (ELISA) method with the specific detection kit (Mlbio, Shanghai, China) following the manufacturer's instructions.

Statistical analysis

Stress treatments were repeated at least twice with three replicates for each line and time point. All data, shown as means ± standard deviation (SD), were processed using SPSS software (SPSS Statistics 17.0, SPSS Inc., Chicago, IL, USA). Analysis of variance (ANOVA) was used to compare the statistical difference based on Fisher's least significant difference test at the significance levels of $P < 0.05$ (*), $P < 0.01$ (**) and $P < 0.001$ (***).

Accession numbers

PtrADC, HQ008237.1; *PtrABF2*, OP187112; *PtrSnRK2.4*, OP187113.

Results

PtrABF2 regulates *PtrADC* by directly binding to its promoter

In our earlier work we have shown that *PtrADC* functions in drought tolerance (Wang *et al*., 2011). To identify upstream TFs regulating *PtrADC*, the trifoliate orange cDNA library was screened by Y1H with a bait constructed using the *PtrADC* promoter (pADC). As a result, two genes encoding either PtrABF2 (C8, Fig. S1) and PtrNAC72 (E8) were successfully identified. PtrNAC72 was found to act as a negative regulator of *PtrADC* (Wu *et al*., 2016). In this study, we first examined the interaction between PtrABF2 and pADC that contains one ABRE element. Y1H assay showed that all of the yeast cells grew well on SD/-Ura/-Leu medium. However, when AbA was added to the medium, only the yeast cells of positive control and those co-transformed with the prey (PtrABF2) and the

bait containing the putative ABRE sequence could survive, whereas no growth was observed in the negative control and those transformed with the prey and the bait harboring a mutated ABRE sequence, from ACGTGG to TTTGTT (Fig. 1a, b), implying that PtrABF2 could bind to pADC. EMSA assay indicated that the promoter fragment harboring the original ABRE element was specifically bound by PtrABF2 protein, suggesting that PtrABF2 could directly bind to the *PtrADC in vitro* (Fig. c). Moreover, ChIP-qPCR analysis using 35S:PtrABF2-GFP transgenic sweet orange calli showed that PtrABF2 bound to pADC *in vivo* through specific association with the promoter region containing the ABRE element (Fig. S2, Fig. 1a, Fig. 1d).

To further elucidate how PtrABF2 affects the expression of *PtrADC*, a dual-Luc reporter assay was performed using tobacco co-transformed with the effector PtrABF2 and the reporter vector constructed using the P1 fragment and its mutated counterpart, mP1. Co-infiltration of the effector and P1-containing reporter led to significant elevation of the promoter activity, which was otherwise resumed to the control level when mP1 was used. The quantitative measurement of LUC activity was also supported by microscopic visualization of the LUC fluorescence signal (Fig. 1e-g). Collectively, these results convincingly demonstrate that PtrABF2 directly binds to the *PtrADC* promoter and transcriptionally activates its expression.

PtrABF2 is a dehydration-induced gene

PtrABF2 transcript levels underwent negligible changes and maintained at low levels in the plants grown under normal conditions. By contrast, *PtrABF2* mRNA abundance was progressively up-regulated by dehydration, reaching the peak level at 9 h. However, the up-regulation of *PtrABF2* was greatly inhibited when fluridone was added before the dehydration treatment (Fig. 2a), implying that the induction of *PtrABF2* by dehydration is ABA-dependent. In addition, exogenous ABA treatment progressively elevated the *PtrABF2* expression levels within 9 h, followed by a decline at the last two time points (Fig. 2b). Putrescine contents in trifoliate orange were increased to reach the highest level at 12 after the dehydration treatment (Fig. 2c). As ABF family contains four members, we also analyzed expression of other three genes, including *PtrABF1*, *PtrABF3* and *PtrABF4*, in trifoliate orange under either dehydration or ABA treatment. Under the dehydration or

ABA treatment, *PtrABF1* mRNA abundance underwent slight change, while those of *PtrABF3* and *PtrABF4* were elevated (Fig. S3a, b). In addition, *PtrABF2* mRNA abundance was slightly up-regulated by salt stress, but exhibited minor repression under the cold treatment (Fig. S4). These results indicated that *PtrABF2* is primarily induced by dehydration and ABA treatment.

PtrABF2 functions as a TF

To identify subcellular localization of PtrABF2, we conducted transient expression of 35S:PtrABF2-YFP in *N. benthamiana* epidermal cells. The 35S: YFP (control vector) generated YFP signals throughout the cells. In contrast, the YFP signal of 35S:PtrABF2-YFP was detected exclusively in the nucleus, and co-localized with the nuclear localization marker VirD2NLS-mCherry (Fig. 3a), indicating that PtrABF2is a nuclear protein, consistent with its role as a transcription factor. To examine whether PtrABF2 has transcription activation activity, we carried out a transactivation reporter assay in yeast cells. Growth assay indicated that the yeast cells transformed with the constructs containing full-length and N-terminal region exhibited normal growth on the selective media, and displayed a galactosidase activity (Fig. 3b-c). These results indicated that the N terminal region is responsible for the transcriptional activity of PtrABF2.

PtrABF2 improves drought tolerance by facilitating putrescine synthesis

The dehydration-induced up-regulation of *PtrABF2* implies that it might function in drought tolerance. To test this hypothesis, lemon transgenic lines overexpressing *PtrABF2* were obtained (Fig. S5). When the wild-type lemon (WT) and the transgenic lines were exposed to drought stress by withholding watering for 25 d and then rewatered for growth recovery, the transgenic lines showed better growth status, as manifested by less leaf wilting and necrosis and stronger chlorophyll fluorescence, as compared with the WT (Fig. 4a-b). We measured EL and MDA, two indicators of damage during abiotic stress, in the tested lines (Huang *et al.*, 2013). Consistent with the enhanced drought tolerance, the transgenic lines had lower EL, MDA and higher Fv/Fm ratios, along with less amount of H_2O_2 and $O_2^{\cdot-}$, than did the WT after the drought stress (Fig. 4c-f). ADC activity and putrescine content in the WT were negligibly lower than those of transgenic plants in the

absence of drought stress. When exposed to the drought treatment, the ADC activity and putrescine content were slightly increased in the WT, but more substantially in the transgenic lines, leading to significant difference between them (Fig. 4g, h). All of these data indicate that overexpression of *PtrABF2* significantly enhanced drought tolerance and promoted putrescine accumulation, particularly under drought stress, in the transgenic plants.

To further investigate the role of PtrABF2 in drought tolerance and putrescine synthesis, we silenced *PtrABF2* in *Poncirus trifoliata* by VIGS. *PtrABF2* expression levels were decreased to different extent in the VIGS plants compared with that of the TRV control (Fig. S6-S7). The plants in which *PtrABF2* was silenced by nearly 60% were then pooled to constitute a VIGS line (designated as TRV-PtrABF2) for drought tolerance assay. No conspicuous difference in plant morphology was detected between the examined plants under normal growth conditions. However, in the presence of drought stress, the VIGS plants displayed more severe leaf wilting and exacerbated loss of turgor, accompanied by repressed chlorophyll fluorescence and lower Fv/Fm ratio, in comparison with the TRV control (Fig. 5a, Fig. S8a, b). In addition, significantly higher levels of EL and MDA were detected in the VIGS line than in the TRV control under the drought stress, but the values were equivalent between each other without the stress condition (Fig. 5b-c). Meanwhile, more H_2O_2 and $O_2^{\cdot-}$ was observed in the VIGS line relative to the TRV control following the drought treatment (Fig. 5d, Fig. S8c, d). We noted that *ADC* expression, ADC activity and putrescine level in the VIGS line were slightly reduced under normal growth conditions, but dramatically decreased under drought stress, relative to the TRV control (Fig. 5e-g). Taken together, these results indicate that silencing of *PtrABF2* inhibited putrescine synthesis and elevated drought susceptibility.

Since the VIGS plants contained less putrescine and showed impaired drought tolerance, we are curious to know whether exogenous supply of putrescine could resume drought tolerance of the VIGS line. To answer this question, we pretreated the VIGS plants with 10 mM putrescine, using water treatment as a control, for 3 d prior to drought exposure. After the drought treatment, the putrescine-pretreated plants displayed prominently less leaf wilting and better chlorophyll fluorescence, along with higher Fv/Fm ratios, than did the water-treated plants (Fig. 5h, Fig. S8e, f). In addition, lower

levels of EL, MDA and ROS (H_2O_2 and $O_2^{\cdot-}$) were observed in the putrescine-pretreated plants (Fig. 5i-k, Fig. S8g, h). Endogenous putrescine levels in the putrescine-supplemented plants were significantly higher than in the water-treated ones under drought implementation (Fig. 5l). These results indicate that exogenous putrescine restored, to some extent, drought tolerance of the VIGS line, implying that putrescine accumulation is involved in *PtrABF2*-mediated drought tolerance.

SnRK2.4 physically interacts with and phosphorylates PtrABF2

It has been previously shown that ABFs are phosphorylated by SnRK2 in an ABA-dependent manner (Umezawa *et al*., 2013; Zhu, *et al*., 2016; Wang *et al*., 2019; Chen *et al*., 2021). A total of seven SnRK2 members, *PtrSnRK2.3*, *PtrSnRK2.4*, *PtrSnRK2.5*, *PtrSnRK2.6*, *PtrSnRK2.7*, *PtrSnRK2.8* and *PtrSnRK2.10* were identified in the *Poncirus trifoliata* genome (Table S2, Fig. S9). We then determined expression patterns of the *PtrSnRK2* genes in response to dehydration and ABA treatment, which showed that *PtrSnRK2.4* exhibited the greatest amplitude of up-regulation by dehydration and ABA treatment, and the expression pattern was consistent with those of *PtrABF2* (Fig. S10). This result allowed us to select *PtrSnRK2.4* for further analysis. Subcellular localization analysis showed that PtrSnRK2.4 is localized to the nucleus and cytoplasm of tobacco epidermis (Fig. S11). We then investigated protein interaction between PtrSnRK2.4 and PtrABF2. Yeast two-hybrid assay showed that PtrSnRK2.4 interacts with PtrABF2 and that the N-terminus of PtrABF2 is responsible for the interaction (Fig. 6a). BiFC assays showed that the two proteins interact in the nucleus of *N. benthamiana* leaves (Fig. 6b). Pull-down analyses using GST/His-tagged fusion proteins further verified the *in vitro* interaction between PtrSnRK2.4 and PtrABF2 (Fig. 6c). Finally, we performed LCIassays to further confirm the interaction between these proteins in tobacco leaves (Fig. 6d). These results strongly indicate that PtrSnRK2.4 and PtrABF2 could form a protein complex.

The interaction between PtrSnRK2.4 and PtrABF2 compelled us to examine whether and how PtrSnRK2.4 phosphorylates PtrABF2. *In vivo* phosphorylation assays by co-expressing HA-PtrSnRK2.4 and GFP-PtrABF2 in *N. benthamiana* leaves and using the antibodies anti-pSer/pThr indicate that PtrSnRK2.4 phosphorylated PtrABF2 in planta (Fig. 7a). The phosphorylation of PtrABF2 by PtrSnRK2 was further confirmed by *in vitro*

kinase assays using purified His-PtrSnRK2.4 and GST-PtrABF2 recombinant proteins (Fig. 7b). LC-MS/MS analysis of the phosphorylated PtrABF2 protein demonstrated that the 93th residue of PtrABF2, serine (Ser93), was a potential phosphorylation site (Fig. 7c, Fig. S12). To confirm this result, Ser93 of PtrABF2 was mutated into Ala, generating PtrABF2^{S93A}, to examine whether it influenced the PtrSnRK2.4-mediated phosphorylation. Strikingly, PtrABF2^{S93A} protein was neither *in vitro* nor *in vivo* phosphorylated by PtrSnRK2.4 (Fig. 7d, e). These results indicate that Ser93 of PtrABF2 was the bona fide target site phosphorylated by PtrSnRK2.4.

Phosphorylation of PtrABF2 is essential for transcriptional regulation of *PtrADC*

To explore the significance of PtrSnRK2.4-mediated PtrABF2 phosphorylation, we first examined whether and how phosphorylation influenced transcriptional activation activity of PtrABF2 by performing the dual LUC assay. The promoter activity was significantly elevated when PtrSnRK2.4 was co-expressed with PtrABF2 in *N. benthamiana* leaves than expressing PtrABF2 alone (Fig. 8a-c). However, the S93A mutation in PtrABF2 completely abolished the induction of promoter activity (Fig. 8d, e). These results indicate that PtrSnRK2.4-mediated phosphorylation at Ser93 is essential for transcriptional activation of PtrABF2. To further validate this conclusion, transgenic calli overexpressing either PtrABF2-GFP or PtrABF2^{S93A}-GFP were produced (Fig. S13). *ADC* expression level, ADC activity and putrescine content were substantially increased in the transgenic callus expressing PtrABF2-GFP relative to the untransformed callus, whereas no drastic difference was noted when PtrABF2^{S93A}-GFP was expressed (Fig. 8f, g, Fig. S14a). In addition, PtrABF2-GFP and PtrABF2^{S93A}-GFP were infiltrated into *N. benthamiana* leaves, in the presence or absence of HA-PtrSnRK2.4, to further explore the effect of PtrABF2 phosphorylation on regulation of *ADC*. ADC activity was significantly higher in the leaves simultaneously expressing PtrABF2 and PtrSnRK2.4 than only expressing PtrABF2. By contrast, the ADC activity and putrescine content in the leaves expressing PtrABF2^{S93A}, irrespective of PtrSnRK2.4 presence, was almost not impacted relative to the control (Fig. 8h, Fig. S14b).

EMSA assay was then performed to investigate whether PtrSnRK2.4-mediated phosphorylation affected the interaction between PtrABF2 and pADC. The binding of

PtrABF2 to the promoter fragment was promoted by including PtrSnRK2.4 in a dosage-dependent manner. Meanwhile, it is noted that S93A mutation in PtrABF2 slightly inhibited its binding to pADC (Fig. 8i). Collectively, these results demonstrate that PtrSnRK2.4-mediated PtrABF2 phosphorylation promoted the transcriptional regulation of *PtrADC*.

PtrSnRK2.4 functions positively in drought tolerance by modulating putrescine accumulation

As *PtrSnRK2.4* was induced by dehydration, efforts were made to unravel its role in drought tolerance. For this purpose, transgenic lemon lines (#2, #6) overexpressing *PtrSnRK2.4* were generated by *Agrobacterium*-mediated transformation, in which endogenous *ABF2* and *ADC* mRNA levels were dramatically elevated relative to WT (Fig. S15). No significant difference in the morphology was observed between the WT and transgenic plants under normal growth conditions. When subjected to the drought conditions by withholding irrigation for 25 d and subsequent 3-d rewatering, the WT exhibited serious leaf wilting, while the transgenic plants remained good growth and leaf turgor (Fig. 9a). The better growth performance of the transgenic plants under drought stress was supported by drastically lower levels of EL, MDA, and ROS, together with stronger chlorophyll fluorescence and higher Fv/Fm ratios (Fig. 9b-f). ADC activity and endogenous putrescine level in the transgenic lines were slightly higher without stressful conditions, but significantly higher upon the drought exposure, than in the WT (Fig. 9g-h).

To further unravel evidence supporting the role of PtrSnRK2.4 in drought tolerance, we silenced *PtrSnRK2.4* (TRV-SnRK2.4) in *Poncirus trifoliata* by VIGS, in which *PtrSnRK2.4* was knocked down by ~75%. It was noted that transcript levels of *PtrSnRK2.6* and *PtrSnRK2.10* underwent minor alteration in the TRV-SnRK2.4 line, implying that the silencing was specific for *PtrSnRK2.4*. By contrast, *PtrABF2* and *PtrADC* were prominently down-regulated in the VIGS line (Fig. S16-S17). When exposed to drought treatment, the TRV-SnRK2.4 plants displayed more serious drought-induced symptoms, such as leaf wilting and chlorosis, relative to the TRV control (Fig. 10a). Consistent with the visual phenotype, significantly higher levels of EL, MDA and

ROS, accompanied by reduced chlorophyll fluorescence and lower Fv/Fm ratio, were detected in the VIGS plants under the drought stress (Fig. 10b-f). In addition, endogenous putrescine content was reduced, slightly without stress and significantly under drought treatment, in the VIGS line relative to the TRV control (Fig. 10g). Interestingly, exogenous supply of putrescine was shown to effectively alleviate drought-induced injuries in the VIGS plants, as revealed by improved plant growth and the examined parameters. These results demonstrate that PtrSnRK2.4 plays a positive role in drought tolerance by modulating, at least in part, the putrescine accumulation.

Discussion

It is known that drought stress can induce accumulation of various metabolites in plant species (Taji *et al*., 2002; Bartels *et al*., 2005; Ming *et al*., 2020). Putrescine, one of the three major PAs, is reported to accumulate in plants exposed to abiotic stresses, including drought, and plays a critical role in combating the stressful environment (Alcázar *et al*., 2010b; Alet *et al*., 2014; Liu *et al*., 2015). Putrescine accumulation under the abiotic stresses is predominantly ascribed to *de novo* synthesis via the ADC pathway (Liu *et al*., 2006; Wu *et al*., 2016). In this regard, *ADC* genes of various plants have been shown to be induced by abiotic stresses, such as drought, salinity, nutrient deficiency, and low temperature (Wang *et al*., 2011; Jang *et al*., 2012; Wu *et al*., 2016; Fu *et al*., 2017). Nevertheless, there is a knowledge gap on regulatory network associated with the *ADC* induction and stress imposition. Therefore, unraveling and deciphering the molecular mechanisms underlying stress-triggered induction of *ADC* genes is important for understanding the putrescine accumulation in response to abiotic stresses. In addition, ABA is a vital signaling molecule that plays a crucial role in orchestrating plant response to drought stress. Although the ABA signaling pathway has been widely illustrated in plants exposed to osmotic stresses, it remains elusive how the components involved in ABA signaling cascade regulate *ADC* expression and putrescine accumulation. In this study, we functionally characterized the ABA-responsive PtrABF2 of *Poncirus trifoliata* as an important transcriptional regulator to modulate drought-induced putrescine synthesis by regulating *PtrADC*. Furthermore, PtrSnRK2.4-mediated phosphorylation of PtrABF2 was shown to be essential for this process.

***PtrADC* is a direct target of PtrABF2**

Increasing evidences show that the ABA signaling cascade is important in the regulation of plant growth and development as well as abiotic stress responses. Currently, the AREB/ABF pathway-mediated stress responses has been extensively and thoroughly investigated to understand the underlying mechanisms. In general, ABFs function as positive regulators by regulating their downstream target genes. So far, a variety of stress-responsive genes have been revealed to be regulated by ABFs in various plants. For example, *RhFer1* was revealed to act as a downstream target of rose RhABF2 that functioned to regulate drought tolerance and iron homeostasis (Liu *et al*., 2017). MeABF of cassava positively regulated the expression of *MeBADH1* and promoted the enrichment of betaine (GB) for maintaining osmotic balance under the drought stress (Feng *et al*., 2019). *Arabidopsis thaliana* ABFs, including ABF1, ABF2 and ABF4, were reported to regulate the expression of Trehalose-6-phosphate phosphatase (*TPPI*), which confers drought resistance and improves WUE by decreasing stomatal apertures and improving root architecture (Lin *et al*., 2020). In addition, AtAREB3/AtDPBF3 could regulate *AtADF5*, a gene associated with stomatal development (Qian *et al*., 2019). Recently, wheat TaABF3 was reported to function in drought tolerance by regulating several drought-related genes, such as *LEA14*, *DREB2A* and *RD29A* (Li *et al*., 2020). In the present study, we demonstrated that PtrABF2 directly and specifically bound to the ABRE element of *PtrADC* and activated its expression, implying that *PtrADC* is a direct target gene of PtrABF2. This result allowed us to establish a regulatory module consisting of ABF2-*ADC* responsible for the putrescine accumulation in response to drought stress. Therefore, we infer that PtrABF2 plays a positive role in regulating putrescine synthesis by activating *PtrADC* expression.

PtrABF2 functions in drought tolerance by modulating putrescine accumulation

So far, the role of ABF2s from various plants in stress tolerance has been extensively illustrated. Overexpression of *Arabidopsis thaliana ABF2* or its homologous genes from other plants has revealed that the ABF2s function as master regulators for abiotic stress tolerance in an ABA-dependent pathway (Guan *et al*., 2009; Hossain *et al*., 2010; Wang

et al., 2021; Zhang *et al*., 2022a). However, it is worth mentioning that the physiological mechanism of the ABF2s in drought tolerance is still poorly understood. Previous studies demonstrated that ABF2s function as positive regulator of drought tolerance possibly by modulating proline biosynthesis, antioxidant activity, water use efficiency and photosynthetic capacity (Zhao *et al*., 2016; Kerr *et al*., 2018). In the current work, overexpression of *PtrABF2* led to significantly increased drought tolerance and putrescine accumulation, whereas knockdown of *PtrABF2* impaired the drought tolerance and putrescine synthesis. Interestingly, application of exogenous putrescine was found to resume the drought tolerance in the *PtrABF2*-silenced plants, implying that drought tolerance magnitude in the tested genotypes was positively correlated with putrescine levels. These results indicate that PtrABF2 might function positively in drought tolerance by modulating the putrescine biosynthesis. Our work provides another line of evidence for understanding the physiological mechanism of ABF2-mediated drought tolerance, due to regulating *ADC*-mediated putrescine accumulation. Putrescine has been recognized as an important compound to counteract abiotic stresses, although the explicit mode of action on its role in stress tolerance remains to be illustrated (Moschou *et al*., 2008; Liu *et al*., 2015). One of the mechanisms underlying putrescine-mediated stress tolerance is attributed to ROS scavenging (Shi *et al*., 2013; Liu *et al*., 2015). It is well known that when exposed to stress conditions plants accumulate more ROS, which causes oxidative stress and damages cellular components (Zhu *et al*., 2020). Accumulating evidence shows that greater levels of putrescine are correlated with a more robust antioxidant system for efficient and powerful scavenging of ROS, which is conducive for maintaining desirable cell growth status under abiotic stresses (Shi *et al*., 2013; Liu *et al*., 2015; Zhao *et al*., 2021). Herein, we noticed that ROS accumulation was substantially alleviated in the transgenic plants overexpressing *PtrABF2*, but dramatically promoted in the *PtrABF2*-silenced plants. In addition, supply of exogenous putrescine profoundly mitigated ROS accumulation in the VIGS line, suggesting that putrescine-triggered ROS scavenging was tightly implicated in *PtrABF2*-mediated drought tolerance. Our findings support the important role of putrescine in modulation of stress tolerance due to ROS detoxification.

PtrSnRK2.4 is both ABA- and drought- responsive

ABA signaling pathway is central for orchestrating the abiotic stress response in higher plants by activating the expression of stress-related genes and relevant physiological metabolism (Lin *et al*., 2021). It has been well documented that the core components involved in ABA signaling cascade, including the ABA receptors, PP2C, SnRK2 and AREB/ABF, work in synergy to relay the stress signal perceived by plant cells to downstream stress response (Zhu *et al*., 2016). Among the components, SnRK2 subfamily members have been demonstrated to play crucial roles in orchestrating the ABA signal when they are released from PP2C-mediated inhibition in the presence of ABA (Li *et al*., 2000; Yoshida *et al*., 2006; Umezawa *et al*., 2010). SnRK2 subfamily contains variable numbers of members in difference plants. Ten *SnRK2* genes have been identified in *Arabidopsis thaliana* and sorghum, while 11 and 12 members were characterized in maize and apple, respectively (Kobayashi *et al*., 2004; Huai *et al*., 2008; Li *et al*., 2010; Shao *et al*., 2014). Nevertheless, the *GhSnRK2* family has 20 members (Liu *et al*., 2017). Surprisingly, only seven SnRK2 subfamily genes were identified in *Poncirus trifoliata*. These results indicate that the number of SnRK2 genes varies among plant species. Variation of gene numbers in the same gene subfamily among different plant species has been widely reported, which may be attributed to gene retraction or diversification, along with the whole-genome duplication (Shao *et al*., 2014). Earlier work has demonstrated that the Group III members of *Arabidopsis thaliana*, including *AtSnRK2.2*, *AtSnRK2.3* and *AtSnRK2.6*, were strongly induced by ABA, drought, and salt, while other members underwent minor changes in the transcriptional levels under drought stress (Fujita *et al*., 2009; Nakashima *et al*., 2009). By contrast, we found that *PtrSnRK2.4* of *Poncirus trifoliata* was profoundly induced by ABA and dehydration treatments. The phylogenetic analysis showed that *PtrSnRK2.4* was most closely related to *MdSnRK2.2/2.4*, *ZmSnRK2.3* and *OsSAPK3*, but not clustered in the same clade as that of *AtSnRK2.4*. *OsSAPK3* was prominently induced by infection of *Xanthomonas oryzae* in rice cultivars carrying the non-host resistance gene *Rxo1*, while *ZmSnRK2.3* and *MdSnRK2.4* were up-regulated in response to drought, NaCl and ABA treatments (Huai *et al*., 2008; Xu *et al*., 2013; Shao *et al*., 2014). These results suggest that the *SnRK2.4* genes in different plants might have undergone functional divergence along with separation of plant lineages. In addition, the findings suggest that the ABA signal might be relayed by various SnRK2

members depending on the plant species.

SnRK2.4-mediated phosphorylation of ABF2 is essential for activation of *ADC* in response to drought

It has been well understood that phosphorylation is an important protein modification at post-transcriptional level, which is a major molecular mechanism underlying the regulation of protein functions in plant response to adverse environment (Zou *et al*., 2015; Kim *et al*., 2017; Gupta *et al*., 2020; Wong *et al*., 2019). Protein phosphorylation is mediated by a diversity of protein kinases, including SnRK2s. Accumulating evidence has demonstrated that SnRK2-mediated phosphorylation of target proteins is tightly involved in regulation of a range of molecular actions associated with the ABA signaling pathway (Fujii *et al*., 2009; Wang *et al*., 2013). Earlier studies have shown that SnRK2.2, SnRK2.3 and SnRK2.6 could phosphorylate AREB1/ABF2, and phosphorylation of Ser45 in AREB1/ABF2 determines whether AREB1 can perform its function normally to regulate the expression of downstream stress-responsive genes (Umezawa *et al*., 2013; Wang *et al*., 2013). Moreover, increasing evidence shows that multiple conserved RXXS/T sites of AREB/ABFs are phosphorylated by SnRK2 protein kinases in an ABA-dependent manner (Uno *et al*. 2000; Fujii *et al*., 2007; Tan *et al*., 2018). However, little is known about the phosphorylation status of ABF2 by SnRK2s during putrescine biosynthesis in the presence of drought conditions. In this study, our data revealed that PtrSnRK2.4 interacts with PtrABF2 to form a heterodimer. In addition, PtrABF2 was experimentally shown to be phosphorylated by PtrSnRK2.4 at Ser93. In-depth work provides evidence to support that PtrSnRK2.4-mediated phosphorylation of PtrABF2 at Ser93 resulted in enhanced binding ability and transactivation activity, implying that the phosphorylation plays a pivotal role in facilitating the transcriptional regulation of PtrABF2 on *PtrADC*. In support of this argument overexpression of *PtrSnRK2.4* led to greater up-regulation of *ADC*, accumulation of putrescine, and enhanced drought tolerance, whereas *PtrSnRK2.4* silencing resulted in opposite results. These findings reveal that Ser93 of PtrABF2 is essential for maintaining its normal function of regulating *ADC* expression and putrescine synthesis in the presence of drought. It is worth mentioning that other proteins also interact with ABFs to regulate drought resistance in plants. For example, DELLA was shown to

interact with ABF2 for modulating drought tolerance, whereas drought tolerance in chrysanthemum depended upon the interaction between BBX19 and ABF3 (Wang *et al*., 2020; Xu *et al*., 2020). Therefore, the possibility that other proteins may form heterodimers with PtrABF2 to co-regulate the ADC pathway cannot be ruled out, and more efforts are required to illustrate the involved proteins to fully understand the regulatory cascade the in future.

In conclusion, we discovered in this study that PtrABF2 directly regulates *PtrADC* expression to modulate putrescine synthesis under drought stress. In addition, PtrSnRK2.4, a Group II member of the SnRK2 subfamily, can interact with and phosphorylate PtrABF2 at the residue Ser93. The PtrSnRK2.4-PtrABF2 complex orchestrates the drought tolerance by governing *ADC*-mediated putrescine accumulation in response to drought cues. Taken together, this study reveals a molecular module composed of PtrSnRK2.4-PtrABF2-*PtrADC* that explains the *ADC* gene induction and putrescine accumulation in plants exposed to drought environment (Figure 11). The findings advance our understanding of the molecular mechanism governing transcriptional regulation of putrescine biosynthesis in response to abiotic stresses.

Acknowledgements

This work was supported by National Key Research and Development Program of China (2018YFD1000300), the National Natural Science Foundation of China (32272644). We thank Prof. Guosheng Xie (Huazhong Agriculture University) and Dr. Pei Jing (Henan Agriculture University) for their assistance in the phosphorylation assays.

Author contributions

J.H.L. conceived and designed the research. J.S., P.S. and W.K. conducted the experiments. J.S. and C.L. analyzed the data. Z.X. provided trifoliate orange seeds. J.S. wrote the manuscript draft. J.H.L. finalized writing and revision of the manuscript. All authors have read and approved the final version of the manuscript. The authors declare no competing interests.

Data availability

The data that support the findings of this study are available from the corresponding author upon reasonable request.

References

Alcázar R, Planas J, SaxenaT, Zarza X, Bortolotti C, Cuevas J, Bitrián M, Tiburcio AF, Altabella T. 2010b. Putrescine accumulation confers drought tolerance in transgenic *Arabidopsis* plants over-expressing the homologous *Arginine decarboxylase 2* gene. *Plant Physiology and Biochemistry* **48**: 547-552.

Alet AI, Sanchez DH, Cuevas JC, Del Valle S, Altabella T, Tiburcio AF, Marro F, Ferrando A, Espasndin FD, Gonzále ME, Ruiz OS. 2014. Putrescine accumulation in *Arabidopsis thaliana* transgenic lines enhances tolerance to dehydration and freezing stress. *Plant Signaling & Behavior* **6**: 278-286.

Bartels D, Sunkar R. 2005. Drought and salt tolerance in plants. *Critical Reviews in Plant Sciences* **24**: 23-58.

Chen L, Zhao Y, Xu S, Zhang Z, Xu Y, Zhang J, Chong K. 2018. OsMADS57 together with OsTB1 coordinates transcription of its target *OsWRKY94* and *D14* to switch its organogenesis to defense for cold adaptation in rice. *New Phytologist* **211**: 599-613.

Chen K, Li GJ, Bressan RA, Song CP, Zhu JK, Zhao Y. 2020. Abscisic acid dynamics, signaling, and functions in plants. *Journal of Integrative Plant Biology* **62**: 25-54.

Chen X, Ding Y, Yang Y, Song C, Wang B, Yang S, Guo Y, Gong Z. 2021. Protein kinases in plant responses to drought, salt, and cold stress. *Journal of Integrative Plant Biology* **63**: 53-78

Cutler SR, Rodriguez PL, Finkelstein RR, Abrams SR. 2010. Abscisic acid: emergence of a core signaling network. *Annual Review of Plant Biology* **61**: 651-679.

Dai WS, Wang M, Gong X, Liu JH. 2018. The transcription factor FcWRKY40 of *Fortunella crassifolia* functions positively in salt tolerance through modulation of ion homeostasis and proline biosynthesis by directly regulating *SOS2* and *P5CS1* homologs. *New Phytologist* **219**: 972-989.

Ding Y, Shi Y, Yang S. 2020. Molecular regulation of plant responses to environmental

temperatures. *Molecular Plant* **13**: 544-564

Feng J, Wang L, Wu Y, Luo Q, Zhang Y, Qiu D, Han J, Su P, Xiong Z, Chang J, Yang G, He G. 2019. *TaSnRK2.9*, a sucrose non-fermenting 1-related protein kinase gene, positively regulates plant response to drought and salt stress in transgenic tobacco. *Frontiers in Plant Science* **9**: 2003.

Furihata T, Maruyama K, Fujita Y, Umezawa T, Yoshida R, Shinozaki K & Yamaguchi-Shinozaki K. 2006. Abscisic acid-dependent multisite phosphorylation regulates the activity of a transcription activator AREB1. *Proceedings of the National Academy of Sciences, USA* **103**: 1988-1993.

Fu XZ, Khan EU, Hu SS, Fan QJ, Liu JH. 2011. Overexpression of the betaine aldehyde dehydrogenase gene from *Atriplex hortensis* enhances salt tolerance in the transgenic trifoliate orange (*Poncirus trifoliata* L. Raf.). *Environmental and Experimental Botany* **74**: 106-113.

Fu Y, Guo C, Wu H, Chen CL. 2017. Arginine decarboxylase *ADC2* enhances salt tolerance through increasing ROS scavenging enzyme activity in *Arabidopsis thaliana*. *Plant Growth Regulation* **83**: 253-263.

Fujii H, Verslues PE, Zhu JK. 2007. Identification of two protein kinases required for abscisic acid regulation of seed germination, root growth, and gene expression in *Arabidopsis*. *Plant Cell* **19**: 485-494.

Fujii H, Zhu JK. 2009. *Arabidopsis* mutant deficient in 3 abscisic acid-activated protein kinases reveals critical roles in growth, reproduction, and stress. *Proceedings of the National Academy of Sciences, USA* **106**: 8380-8385.

Fujita Y, Yoshida T. & Yamaguchi-Shinozaki K. 2013. Pivotal role of the AREB/ABF-SnRK2 pathway in ABRE-mediated transcription in response to osmotic stress in plants. *Physiologia Plantarum* **147**: 15-27.

Fujita Y, Nakashima K, Yoshida T, Katagiri T, Kidokoro S, Kanamori N. & Kobayashi M. 2009. Three SnRK2 protein kinases are the main positive regulators of abscisic acid signaling in response to water stress in *Arabidopsis*. *Plant and Cell Physiology* **50**: 2123-2132.

Ge W, Luo M, Sun H, Wei B, Zhou X, Zhou Q, Ji S. 2022. The CaMYB340 transcription factor induces chilling injury in post-harvest bell pepper by inhibiting

fatty acid desaturation. *Plant Journal* **111**: 800-818.

Gong X, Zhang J, Hu J, Wang W, Wu H, Zhang Q, Liu JH. 2015. FcWRKY70, a WRKY protein of *Fortunella crassifolia*, functions in drought tolerance and modulates putrescine synthesis by regulating arginine decarboxylase gene. *Plant Cell & Environment* **38**: 2248-2262.

Gou JY, Felippes FF, Liu CJ, Weigel D, Wang JW 2011. Negative regulation of anthocyanin biosynthesis in *Arabidopsis* by a miR156-targeted SPL transcription factor. *Plant Cell* **23**: 1512-1522.

Guan Y, Ren H, Xie H, Ma Z, Chen F. 2009. Identification and characterization of bZIP-type transcription factors involved in carrot (*Daucus carota* L.) somatic embryogenesis. *Plant Journal* **60**: 207-217.

Gupta A, Rico-Medina A, Cano-Delgado AI. 2020. The physiology of plant responses to drought. *Science* **368**: 266-269.

Gupta KJ, Kolbert Z, Durner J, Lindermayr C, Corpas FJ, Brouquisse R, Barroso JB, Umbreen S, Palma JM, Hancock JT, et al. 2020. Regulating the regulator: nitric oxide control of post-translational modifications. *New Phytologist* **227**: 1319-1325.

Hellens RP, Allan AC, Friel EN, Bolitho K, Grafton K, Templeton MD, Karunairetnam S, Gleave AP, Laing WA. 2005. Transient expression vectors for functional genomics, quantification of promoter activity and RNA silencing in plants. *Plant Methods* **1**: 13.

Hossain MA, Cho JI, Han M, Ahn CH, Jeon JS, An G, Park PB. 2010. The ABRE-binding bZIP transcription factor OsABF2 is a positive regulator of abiotic stress and ABA signaling in rice. *Journal of Plant Physiology* **167**: 1512-1520.

Hu Z, Li J, Ding S, Cheng F, Li X, Jiang Y, Yu J, Foyer CH, Shi K. 2021. The protein kinase CPK28 phosphorylates ascorbate peroxidase and enhances thermotolerance in tomato. *Plant Physiology* **186**: 1302-1317.

Hu T, Ye J, Tao P, Li H, Zhang J, Zhang Y, Ye Z. 2016. The tomato HD-Zip I transcription factor SlHZ24 modulates ascorbate accumulation through positive regulation of the D-mannose/L-galactose pathway. *Plant Journal* **85**: 16-29.

Huai J, Wang M, He J, Zheng J, Dong Z, Lv H, Zhao J, Wang G. 2008. Cloning and

characterization of the SnRK2 gene family from *Zea mays*. *Plant Cell Reports* **27**: 1861-1868.

Huang XS, Wang W, Zhang Q, Liu JH. 2013. A basic helix-loop-helix transcription factor, PtrbHLH, of *Poncirus trifoliata* confers cold tolerance and modulates peroxidase-mediated scavenging of hydrogen peroxide. *Plant Physiology* **162**: 1178-1194.

Hyunhee Joo, Chae Woo Lim, Sung Chul Lee. 2019. Roles of pepper bZIP transcription factor CaATBZ1 and its interacting partner RING-type E3 ligase CaASRF1 in modulation of ABA signalling and drought tolerance. *Plant Journal* **100**: 399-410.

Jang SJ, Wi SJ, Choi YJ, An G, Park KY. 2012. Increased polyamine biosynthesis enhances stress tolerance by preventing the accumulation of reactive oxygen species: T-DNA mutational analysis of *Oryza sativa* lysine decarboxylase-like protein 1. *Molecules and Cells* **34**: 251-262.

Kerr TC, Abdel‐Mageed H, Aleman L, Lee J, Payton P, Cryer D, Allen RD. 2018. Ectopic expression of two *AREB/ABF* orthologs increases drought tolerance in cotton (*Gossypium hirsutum*). *Plant Cell & Environment* **41**: 898-907.

Kim SH, Kim HS, Bahk S, An J, Yoo Y, Kim JY, Chung WS. 2017. Phosphorylation of the transcriptional repressor MYB15 by mitogen-activated protein kinase 6 is required for freezing tolerance in *Arabidopsis*. *Nucleic Acids Research* **45**: 6613-6627.

Kobayashi Y, Murata M, Minami H, Yamamoto S, Kagaya Y, Hobo T, Yamamoto A. & Hattori T. 2005. Abscisic acid-activated SnRK2 protein kinases function in the gene-regulation pathway of ABA signal transduction by phosphorylating ABA response element-binding factors. *Plant Journal* **44**: 939-949.

Kobayashi Y, Yamamoto S, Minami H, Kagaya Y, Hattori T. 2004. Differential activation of the rice sucrose nonfermenting1-related protein kinase 2 family by hyperosmotic stress and abscisic acid. *Plant Cell* **16**: 1163-1177.

Li F, Mei F, Zhang Y, Li S, Kang Z, Mao H. 2020. Genome-wide analysis of the *AREB/ABF* gene lineage in land plants and functional analysis of *TaABF3* in *Arabidopsis*. *BMC Plant Biology* **20**: 1-15.

Li J, Wang X, Watson MB, Assmann SM. 2000. Regulation of abscisic acid-induced

stomatal closure and anion channels by guard cell AAPK kinase. *Science* **287**: 300-303.

Li J, Zeng Y, Pan Y, Zhou L, Zhang Z, Guo H, Lou Q, Shui G, Huang H, et al. 2021. Stepwise selection of natural variations at CTB2 and CTB4a improves cold adaptation during domestication of japonica rice. *New Phytologist* **231**: 1056-1072.

Li LB, Zhang YR, Liu KC, Ni, ZF, Fang ZJ, Sun, QS, Gao JW. 2010. Identification and bioinformatics analysis of SnRK2 and CIPK family genes in Sorghum. *Agricultural Sciences in China* **9**: 19-30.

Lin Q, Wang S, Dao Y, Wang J, Wang K. 2020. *Arabidopsis thaliana* trehalose-6-phosphate phosphatase gene *TPPI* enhances drought tolerance by regulating stomatal apertures. *Journal of Experimental Botany* **71**: 4285-4297.

Lin Z, Li Y, Wang Y, Liu X, Ma L, Zhang Z, Mu C, Zhang Y, Peng L, Xie S, Song CP, Shi H, Zhu JK, Wang P. 2021. Initiation and amplification of SnRK2 activation in abscisic acid signaling. *Nature Communications* **12**: 2456.

Liu J, Fan Y, Zou J, Fang Y, Wang L, Wang M, Jiang X, Liu Y, Gao J, Zhang C. 2017. A RhABF2/Ferritin module affects rose (*Rosa hybrida*) petal dehydration tolerance and senescence by modulating iron levels. *Plant Journal* **92**: 1157-1169.

Liu JH, Nada K, Honda C, Kitashiba H, Wen XP, Pang XM. 2006. Polyamine biosynthesis of apple callus under salt stress: importance of the arginine decarboxylase pathway in stress response. *Journal of Experimental Botany* **57**: 2589-2599.

Liu JH, Peng T, Dai W. 2014. Critical *cis*-acting elements and interacting transcription factors: key players associated with abiotic stress responses in plants. *Plant Molecular Biology Reporter* **32**: 303-317.

Liu JH, Wang W, Wu H, Gong X, Moriguchi T. 2015. Polyamines function in stress tolerance: from synthesis to regulation. *Frontiers in Plant Science* **6**: 827.

Liu YJ, Gao N, Ma QJ, Zhang JC, Wang X, Lu J, Hao YJ, Wang XF, You CX. 2021. The MdABI5 transcription factor interacts with the *MdNRT1.5/MdNPF7.3* promoter to fine-tune nitrate transport from roots to shoots in apple. *Horticulture Research* **8**: 236.

Liu Z, Ge X, Yang Z. 2017. Genome-wide identification and characterization

of SnRK2 gene family in cotton (*Gossypium hirsutum* L.). *BMC Genetics* **18**: 54.

Livak KJ, Schmittgen TD. 2001. Analysis of relative gene expression data using real-time quantitative PCR and the $2^{(-\Delta\Delta CT)}$ method. *Methods* **25**: 402-408.

Lyzenga WJ, Stone SL. 2012. Abiotic stress tolerance mediated by protein ubiquitination. *Journal of Experimental Botany* **63**: 599.

Ma Y, Szostkiewicz I, Korte A, Moes D, Yang Y. 2009. Regulators of PP2C phosphatase activity function as abscisic acid sensors. *Science* **324**: 1064.

Ma QJ, Sun MH, Lu J, Liu YJ, You CX, Hao YJ. 2017a. An apple CIPK protein kinase targets a novel residue of AREB transcription factor for ABA-dependent phosphorylation. *Plant Cell & Environment* **40**: 2207-2219.

Ma QJ, Sun MH, Lu J, Liu YJ, Hu DG, Hao YJ. 2017b. Transcription factor AREB2 is involved in soluble sugar accumulation by activating sugar transporter and amylase genes. *Plant Physiology* **174**: 2348-2362.

Mao WW, Han Y, Chen YT, Sun MZ, Feng QQ, Li L, Liu LP, Zhang KK, Wei LZ, Han ZH, Li BB. 2022. Low temperature inhibits anthocyanin accumulation in strawberry fruit by activating FvMAPK3-induced phosphorylation of FvMYB10 and degradation of Chalcone Synthase 1. *Plant Cell* **34**: 1226-1249.

Meng L, Zhang QH, Yang J, Xie GS, Liu JH. 2020. PtrCDPK10 of *Poncirus trifoliata* functions in dehydration and drought tolerance by reducing ROS accumulation via phosphorylating *PtrAPX*. *Plant Science* **291**:110320.

Ming R, Zhang Y, Wang Y, Khan M, Dahro B, Liu, JH. 2020. The JA responsive MYC2-*BADH-like* transcriptional regulatory module in *Poncirus trifoliata* contributes to cold tolerance by modulation of glycine betaine biosynthesis. *New Phytologist* **229**: 2730-2750.

Mohapatra S, Minocha R, Long S, Subhash C Minocha SC. 2009. Putrescine overproduction negatively impacts the oxidative state of poplar cells in culture. *Plant Physiology and Biochemistry* **47:** 262-271.

Moschou PN, Paschalidis KA, Roubelakis-Angelakis KA. 2008. Plant polyamine catabolism: The state of the art. *Plant Signaling Behavior* **3:** 20161-1066.

Nakashima K, Fujita Y, Kanamori N, Katagiri T, Umezawa T, Kidokoro S, Maruyama K, et al. 2009. Three *Arabidopsis* SnRK2 protein kinases, SRK2D/

SnRK2.2, SRK2E/SnRK2.6/OST1 and SRK2I/SnRK2.3, involved in ABA signaling are essential for the control of seed development and dormancy. *Plant & Cell Physiology* **50**: 1345-1363.

Paschalidis KA, Roubelakis-Angelakis KA. 2005. Spatial and temporal distribution of polyamine levels and polyamine anabolism in different organs/tissues of the tobacco plant: correlations with age, cell division/expansion, and differentiation. *Plant Physiology* **138**: 142-152.

Park SY, Fung P, Nishimura N, Jensen DR, Fujii H. 2009. Abscisic acid inhibits type 2C protein phosphatases via the PYR/PYL family of START proteins. *Science* **324**: 1068-1071.

Qian D, Zhang Z, He J, Zhang P, Ou X, Li T, Niu L, Nan Q, Niu Y, He W, An L, Jiang K, Xiang Y. 2019. *Arabidopsis ADF5* promotes stomatal closure by regulating actin cytoskeleton remodeling in response to ABA and drought stress. *Journal of Experimental Botany* **70**: 435-446.

Reyes JL. 2010. Post-transcriptional gene regulation of salinity and drought responses by plant micro-RNAs. *Plant Cell & Environment* **33**: 481-489.

Saruhashi M, Kumar Ghosh T, Arai K, Ishizaki Y, Hagiwara K, Komatsu K, et al. 2015. Plant Raf-like kinase integrates abscisic acid and hyperosmotic stress signaling upstream of SNF1-related protein kinase2. *Proceedings of the National Academy of Sciences, USA* **112**: E6388-6396.

Shao Y, Qin Y, Zou YJ, Ma FW. 2014. Genome-wide identification and expression profiling of the SnRK2 gene family in *Malus prunifolia*. *Gene* **552**: 87-97.

Shi H, Ye T, Chen F, Cheng Z, Wang Y, Yang P, Zhang Y, Chan Z. 2013. Manipulation of arginase expression modulates abiotic stress tolerance in *Arabidopsis*: effect on arginine metabolism and ROS accumulation. *Journal of Experimental Botany* **64**: 1367-1379.

Shi H, Chan Z. 2014. Improvement of plant abiotic stress tolerance through modulation of the polyamine pathway. *Journal of Integrative Plant Biology* **56**: 114-121.

Song J, Wu H, He F, Qu J, Wang Y, Li CL, Liu JH. 2022. *Citrus sinensis* CBF1 functions in cold tolerance by modulating putrescine biosynthesis through regulation of arginine decarboxylase. *Plant and Cell Physiology* **63**:19-29.

Song L, Huang SC, Wise A, Castanon R, Nery JR, Chen H, Watanabe M, Thomas J, Bar-Joseph Z, Ecker JR. 2016. A transcription factor hierarchy defines an environmental stress response network. *Science* **354**: aag1550.

Song, Y; Zhang, XY; LI MZ, Yang H, Fu DY, Lv J, Ding YL, Gong ZZ, Shi YT Yang, SH. 2021. The direct targets of CBFs: In cold stress response and beyond. *Journal of Integrative Plant Biology* 63: 1868-1887.

Soon FF, Ng LM, Zhou XE, West GM, Kovach A, Tan MH, Suino-Powell KM, et al. 2012. Molecular mimicry regulates ABA signaling by SnRK2 kinases and PP2C phosphatases. *Science* **335**: 85-88.

Sun P, Zhu X, Huang X, Liu JH. 2014. Overexpression of a stress responsive MYB transcription factor of *Poncirus trifoliata* confers enhanced dehydration tolerance and increases polyamine biosynthesis. *Plant Physiology and Biochemistry* **78**: 71-79.

Taji T, Ohsumi C, Iuchi S, Seki M, Kasuga M, Kobayashi M, Yamaguchi-Shinozaki K. & Shinozaki K. 2002. Important roles of drought-and cold-inducible genes for galactinol synthase in stress tolerance in *Arabidopsis thaliana*. *Plant Journal* **29**: 417-426.**Takahashi Y, Zhang J, Hsu PK, Ceciliato PHO, Zhang L, Dubeaux G, Munemasa S, Ge C, Zhao Y, Hauser F, Schroeder JI. 2020.** MAP3Kinase-dependent SnRK2-kinase activation is required for abscisic acid signal transduction and rapid osmotic stress response. *Nature Communications* **11:**12.

Tan W, Zhang D, Zhou H, Zheng T, Yin Y, Lin H. 2018. Transcription factor HAT1 is a substrate of SnRK2.3 kinase and negatively regulates ABA synthesis and signaling in *Arabidopsis* responding to drought. *PLoS Genetics* **14**: e1007336.

Tsaniklidis G, Pappi P, Tsafouros A, Charova SN, Nikoloudakis N, Roussos PA, Paschalidis KA, Delis C. 2020. Polyamine homeostasis in tomato biotic/abiotic stress cross-tolerance. *Gene* **727**: 144230.

Umezawa T, Sugiyama N, Takahashi F, Anderson JC, Ishihama Y, Peck SC. & Shinozaki K. 2013. Genetics and phosphoproteomics reveal a protein phosphorylation network in the abscisic acid signaling pathway in *Arabidopsis thaliana*. *Science Signaling* **6**: rs8-rs8.

Umezawa T, Nakashima K, Miyakawa T, Kuromori T, Tanokura M, Shinozaki K, Yamaguchi-Shinozaki K. 2010. Molecular basis of the core regulatory network in

ABA responses: sensing, signaling and transport. *Plant and Cell Physiology* **51**: 1821-1839.

Uno Y, Furihata T, Abe H, Yoshida R, Shinozaki K, Yamaguchi-Shinozaki K. 2000. *Arabidopsis* basic leucine zipper transcription factors involved in an abscisic acid-dependent signal transduction pathway under drought and high-salinity conditions. *Proceedings of the National Academy of Sciences, USA* **97**:11632-11637.

Wang J, Sun PP, Chen CL, Wang Y, Fu XZ, Liu JH. 2011. An arginine decarboxylase gene *PtADC* from *Poncirus trifolita* confers abiotic stress tolerance and promotes primary root growth in *Arabidopsis*. *Journal of Experimental Botany* **62**: 2899-2914.

Wang W, Konstantinos P, Feng J, Song J, Liu JH. 2019. Polyamine catabolism in plants: a universal process with diverse functions. *Frontiers in Plant Science* **10**: 561.

Wang RK, Li LL, Cao ZH, Zhao Q, Li M, Zhang LY. & Hao YJ. 2012. Molecular cloning and functional characterization of a novel apple *MdCIPK6L* gene reveals its involvement in multiple abiotic stress tolerance in transgenic plants. *Plant Molecular Biology* **79**: 123-135.

Wang P, Xue L, Batelli G, Lee S, Hou YJ, et al. 2013. Quantitative phosphoproteomics identifies SnRK2 protein kinase substrates and reveals the effectors of abscisic acid action. *Proceedings of the National Academy of Sciences, USA* **110**: 11205-11210.

Wang X, Guo C, Peng J, Li C, Wan F, Zhang S, Zhou Y, Yan Y, Qi L, Sun K. 2019. ABRE-binding factors play a role in the feedback regulation of ABA signaling by mediating rapid ABA induction of ABA co-receptor genes. *New Phytologist* **221**: 341-355.

Wang YH, Que F, Li T, Zhang RR, Khadr A, Xu ZS, Tian YS, Xiong AS. 2021. DcABF3, an ABF transcription factor from carrot, alters stomatal density and reduces ABA sensitivity in transgenic *Arabidopsis*. *Plant Science* **302**: 110699.

Wang Y, Feng C, Zhai Z, Peng X, Wang Y, Sun Y, Li J, Shen X, Xiao Y, Zhu S, Huang X, Li T. 2020. The apple microR171i-scarecrow-like proteins26.1 module enhances drought stress tolerance by integrating ascorbic acid metabolism. *Plant Physiology* 184: 194-211.

Wang Z, Liu L, Cheng C, Ren Z, Xu S, Li X. 2020. *GAI* functions in the plant response to dehydration stress in *Arabidopsis thaliana*. *International Journal of Molecular*

Sciences **21**: 819.

Wong MM, Bhaskara GB, Wen TN, Lin WD, Nguyen TT, Chong GL, Verslues PE. 2019. Phosphoproteomics of *Arabidopsis* highly ABA induced 1 identifies AT-hook-like10 phosphorylation required for stressgrowth regulation. *Proceedings of the National Academy of Sciences, USA* **116**: 2354-2363.

Wu H, Fu B, Sun P, Xiao C, Liu JH. 2016. A NAC transcription factor represses putrescine biosynthesis and affects drought tolerance. *Plant Physiology* **172**: 1532-1547.

Xu MR, Huang LY, Zhang F, Zhu LH, Zhou YL, Li ZK. 2013. Genome-wide phylogenetic analysis of stress-activated protein kinase genes in rice (OsSAPKs) and expression profiling in response to *Xanthomonas oryzae* pv. *oryzicola* infection. *Plant Molecular Biology Reporter* **31**: 877-885.

Xu Y, Zhao X, Aiwaili P, Mu X, Zhao M, Zhao J, Cheng L, Ma C, Gao J, Hong B. 2020. A zinc finger protein BBX19 interacts with ABF3 to affect drought tolerance negatively in chrysanthemum. *Plant Journal* **103**: 1783-1795.

Yang T, Wang H, Guo L, Wu X, Xiao Q, Wang J, Wang Q, Ma G, Wang W, Wu Y. 2022. ABA-induced phosphorylation of basic leucine zipper 29, ABSCISIC ACID INSENSITIVE 19, and Opaque2 by SnRK2.2 enhances gene transactivation for endosperm filling in maize. *Plant Cell* **34**:1933-1956.

Yoshida T, Fujita Y, Maruyama K, Mogami J, Todaka D, Shinozaki K, Yamaguchi-Shinozaki K. 2015. Four *Arabidopsis* AREB/ABF transcription factors function predominantly in gene expression downstream of SnRK2 kinases in abscisic acid signaling in response to osmotic stress. *Plant Cell & Environment* **38**: 35-49.

Yoshida R, Umezawa T, Mizoguchi T, Takahashi S, Takahashi F, Shinozaki K. 2006. The regulatory domain of SRK2E/OST1/SnRK2.6 interacts with ABI1 and integrates abscisic acid (ABA) and osmotic stress signals controlling stomatal closure in *Arabidopsis. Journal of Biological Chemistry* **281**: 5310-5318.

Zandalinas SI, Mittler R. 2022. Plant responses to multifactorial stress combination. *New Phytologist* **234**: 1161-1167.

Zandalinas SI, Mittler R, Balfagón D, Arbona V, Gómez-Cadenas A. 2018. Plant adaptations to the combination of drought and high temperatures. *Physiologia*

Plantarum 162: 2-12.

Zandalinas SI, Balfagón D, Gómez-Cadenas A, Mittler R. 2022. Responses of plants to climate change: Metabolic changes during abiotic stress combination in plants. *Journal of Experimental Botany* 73: 3339-3354.

Zhang H, Mao L, Xin M, Xing H, Zhang Y, Wu J, Xu D, Wang Y, Shang Y, Wei L, Cui M, Zhuang T, Sun X, Song X. 2022a. Overexpression of *GhABF3* increases cotton (*Gossypium hirsutum* L.) tolerance to salt and drought. *BMC Plant Biology* **22**: 313.

Zhang H, Zhu J, Gong Z, Zhu JK. 2022b. Abiotic stress responses in plants. *Nature Reviews Genetics* **23**: 104-119.

Zhang Q, Wang M, Hu J, Wang W, Fu X, Liu JH. 2015. *PtrABF* of *Poncirus trifoliata* functions in dehydration tolerance by reducing stomatal density and maintaining reactive oxygen species homeostasis. *Journal of Experimental Botany* **66**: 5911-5927.

Zhao BY, Hu YF, Li JJ, Yao X, Liu KD. 2016. BnaABF2, a bZIP transcription factor from rapeseed (*Brassica napus* L.), enhances drought and salt tolerance in transgenic *Arabidopsis*. *Botanical Studies* **57**: 12.

Zhao JQ, Wang XF, Pan XB, Jiang Q, Xi ZM. 2021. Exogenous putrescine alleviates Drought stress by altering reactive oxygen species scavenging and biosynthesis of polyamines in the seedlings of *Cabernet Sauvignon*. *Frontiers in Plant Science* **12:** 767992.

Zhao M, Zhang N, Gao T, Jin J, Jing T, Wang J, Wu Y, Wan X, Schwab W, Song C. 2020. Sesquiterpene glucosylation mediated by glucosyltransferase UGT91Q2 is involved in the modulation of cold stress tolerance in tea plants. *New Phytologist* **226**: 362-372.

Zhao S, Gao H, Jia X, Wei J, Mao K, Ma F. 2021. *MdHB-7* Regulates Water Use Efficiency in Transgenic Apple (*Malus domestica*) Under Long-Term Moderate Water Deficit. *Frontiers in Plant Science* **12**: 740492.

Zhao Y, Zhang Z, Gao J, Wang P, Hu T, Wang Z, et al. 2018. *Arabidopsis* duodecuple mutant of PYL ABA receptors reveals PYL repression of ABA-independent SnRK2 activity. *Cell Reports* **23**: 3340-3351.

Zhou JG, Liu DR, Wang P, Ma XY, Lin WW, Cheng SX, Mishev K, Lu DP, Kumar

R, Vanhoutte I, et al. 2018. Regulation of *Arabidopsis* brassinosteroid receptor BRI1 endocytosis and degradation by plant U-box PUB12/PUB13-mediated ubiquitination. *Proceedings of the National Academy of Sciences, USA* **115**: E1906-E1915.

Zhu H, Chen C, Zeng J, Yun Z, Liu Y, Qu H, Jiang Y, Duan X, Xia R. 2020. *MicroRNA528*, a hub regulator modulating ROS homeostasis via targeting of a diverse set of genes encoding copper-containing proteins in monocots. *New Phytologist* **225**: 385-399.

Zhu JK. 2002. Salt and drought stress signal transduction in plants. *Annual Review of Plant Boilogy* **53**: 247.

Zhu, JK. 2016. Abiotic stress signaling and responses in plants. *Cell* **167**: 313-324.

Zou JJ, Li XD, Ratnasekera D, Wang C, Liu WX, Song LF, Zhang WZ, Wu WH. 2015. *Arabidopsis* calcium-dependent protein kinase 8 and catalase 3 function in abscisic acid-mediated signaling and H_2O_2 homeostasis in stomatal guard cells under drought stress. *Plant Cell* **27**: 1445-1460.

Figure Legends

Fig. 1. PtrABF2 directly binds to and activates the promoter of *PtrADC*. (a) Schematic diagrams of *PtrADC* promoter, the bait and prey constructs used for Y1H assay. The red triangle indicates the ABRE element within the promoter fragment (P1). Grey bars indicate the three regions (F1, F2, F3) used for ChIP-qPCR analysis. (b) Growth of yeast cells transformed with prey (pGADT7-PtrABF2) and bait (P1 or mP1), along with negative control (bait+pGADT7) and positive control (p53-AbAi+ pGAD-p53), on selective medium without (left) or with (right) AbA (200 ng mL^{-1}). (c) EMSA assay for examination of interaction between PtrABF2 and *PtrADC* promoter. The His-PtrABF2 protein was incubated with the biotin-labeled probes containing wild-type ABRE element (ACGTGG) or its mutated sequence (TTTGTT), along with or without the unlabeled competitor at 10× and 100× molar excess. The red and black arrowheads indicate bound and free probes, respectively. + and -, presence or absence of the component. (d) Enrichment of PtrABF2 in the regions of *PtrADC* promoter, as revealed by ChIP-qPCR. Actin was used as the internal control. (e) Schematic diagram of the effector and reporter constructs used for dual luciferase (LUC) assays. MCS, multiple cloning sites. P_{35S} and T_{35S} are promoter and terminator of CaMV *35S*, respectively. LUC and REN are firefly luciferase and *Renilla luciferase*, respectively. (f) Promoter activity analysis, based on LUC/REN ratio, in different combinations of effector and reporter. LUC/REN ratio of SK-PtrABF2/pGreen II 0800 was set to 1 for normalization. Data in (d, f) are shown as means ± SE (n = 3). Asterisks indicate that the value is significantly different from that of the control (***$P < 0.001$), based on a one-way Fisher's least significant difference test. (g) A representative bioluminescence image for LUC signals of the tobacco leaf sections infiltrated with the designated effectors and reporters.

Fig. 2. Expression patterns of *PtrABF2* in response to dehydration and abscisic acid (ABA) treatment. (a) *PtrABF2* transcript levels in trifoliate orange seedlings under normal growth conditions, or subjected to dehydration with or without fluridone

pretreatment. (b) *PtrABF2* expression levels in trifoliate orange seedlings incubated in 100 μM ABA solution. Leaves were collected at the designated time points for expression analysis. (c) Putrescine levels in trifoliate orange plants under dehydration conditions. FW, fresh weight. *Actin* was used as an internal control. Error bars indicate ± SE (n = 3).

Fig. 3. Subcellular localization and transcriptional activation of PtrABF2. (a) Confocal microscopic images taken under bright field, or fluorescence emission wavelength for YFP or mCherry. The overlays are shown on the right. The constructs, along with a nucleus marker gene VirD2NLS fused to mCherry, were infiltrated into *Nicotiana benthamiana* leaves. (b) Schematic diagrams of the constructs used for transcriptional activation activity assays. Full-length (PtrABF2) and truncated halves, PtrABF2-N (N-terminal fragment) and PtrABF2-C (C-terminal fragment), were fused to the GAL4 DNA-binding domain in pGBKT7. The numbers indicate the amino acid positions (c) Growth of yeast cells co-transformed with different vectors on selective medium, using pGBKT7-53 + pGADT7-T as a positive control and pGBKT7 as a negative control.

Fig. 4. Overexpression of *PtrABF2* confers significantly enhanced drought tolerance in transgenic lemon.

(a) Phenotype of transgenic and wild type (WT) lemon plants before and after the drought treatment. Plants were deprived of watering for 25 d, then rewatered and grew for another 3 d. Scale bars = 2 cm. (b-e) chlorophyll fluorescence (b), electrolyte leakage (c), MDA content (d), Fv/Fm ratios (e) in the tested lines before and after the drought treatment. (f) *In situ* detection of H_2O_2 and $O_2^{\cdot -}$ in the tested lines after drought treatment. (g-h) ADC activity (g) and putrescine content (h) in the tested lines before and after drought treatment. FW, fresh weight. Data in (c, d, e, g, h) are shown as means ± SE (n = 3). Asterisks indicate significant difference between the transgenic lines and WT under drought stress (**P < 0.01, ***P < 0.001), based on a one-way Fisher's least significant difference test.

Fig. 5. Knockdown of *PtrABF2* in *Poncirus trifoliata* by VIGS increases drought sensitivity.

(a) Phenotypes of VIGS line (TRV-PtrABF2) and TRV control before and after drought treatment. Scale bars = 2 cm. (b-g) Electrolyte leakage (b), MDA content (c), *in situ* accumulation of $O_2^{\cdot-}$ and H_2O_2 (d), relative expression level of *PtrADC* (e), ADC activity (f) and endogenous putrescine content (g) in the VIGS line and TRV control before and after drought treatment. (h) Phenotype of the VIGS plants, pretreated with water or 10 mM putrescine, after drought treatment. Scale bars, 2 cm. (i-l) Electrolyte leakage (i), MDA content (j), *In situ* accumulation of H_2O_2 and $O_2^{\cdot-}$ (k) and endogenous putrescine content (l) in the water- or putrescine-pretreated VIGS plants before and after the drought treatment. FW indicates fresh weight. Data in (b, c, e, f, g, i, j, l) are shown as means ± SE (n = 3). Asterisks indicate significant difference between different groups under the same conditions (** $P < 0.01$, *** $P < 0.001$), based on a one-way Fisher's least significant difference test.

Fig. 6. PtrSnRK2.4 physically interacts with PtrABF2 *in vitro* and *in vivo*.

(a) Y2H assays demonstrating the interaction of PtrSnRK2.4 and PtrABF2. Growth of yeast cells co-transformed with different vectors on SD/-Trp-Leu and SD/-Trp-Leu-His-Ade/+Aba (100 ng mL^{-1}) with X-α-gal, using pGBKT7-53 + pGADT7-T as a positive control and pGBKT7 + pGADT7-SnRK2.4 as a negative control. (b) BiFC analysis shows the interaction between SnRK2.4 and ABF2 in the nucleus. *N. benthamiana* leaves transiently expressing the designated vectors were subjected to confocal microscopic observation of YFP fluorescence signals. Scale bar = 25 μm. (c) Pull-down assays confirming the *in vitro* interaction between PtrSnRK2.4 and PtrABF2. His-PtrSnRK2.4 was incubated with GST-PtrABF2 immobilized on GST beads. His-PtrSnRK2.4 and GST-PtrABF2 were detected using antibodies anti-His and anti-GST, respectively. GST protein was used as the control. (d) LCI assay for examining the interaction between PtrSnRK2.4 and PtrABF2, based on LUC signals in the leaf sections infiltrated with the designated constructs.

Fig. 7. PtrSnRK2.4 phosphorylates PtrABF2 at Ser93 residue.

(a) PtrSnRK2.4 phosphorylates PtrABF2 *in vivo*. *N. benthamiana* leaves co-expressing PtrABF2-GFP and HA-PtrSnRK2.4 were subjected to protein immunoprecipitation using

the anti-GFP antibody, followed by immunoblotting with anti-pSer/pThr and anti-GFP antibodies. HA-PtrSnRK2.4 protein was detected by anti-HA antibody. (b) PtrSnRK2.4 phosphorylates PtrABF2 *in vitro*. His-PtrSnRK2.4 was incubated with GST-PtrABF2 in a kinase buffer at 30 °C for 30 min. The phosphorylated protein was detected by autoradiography. GST-ABF2 was detected by anti-pSer/pThr and anti-GST antibody, while His-PtrSnRK2.4 was detected by anti-His antibody. (c) Detection of phosphorylated amino acid residue in PtrABF2 by LC-MS/MS. b and y with numbers represent the N-terminal and C-terminal ions, respectively, of the peptide with retained charge. The m/z indicates mass charge ratio. (d, e) Detection of phosphorylation status of PtrABF2 or PtrABF2^{S93A} by PtrSnRK2.4. HA-PtrSnRK2.4 was infiltrated with either PtrABF2-GFP or PtrABF2^{S93A}-GFP into *N. benthamiana* leaves (d). His-PtrSnRK2.4 was incubated with GST-PtrABF2 or GST- PtrABF2^{S93A} in a kinase buffer at 30 °C for 30 min (e).

Fig. 8. PtrSnRK2.4-mediated phosphorylation of PtrABF2 enhances transcriptional regulation.

(a) Schematic diagram of the effector and reporter constructs used for dual luciferase (LUC) assays. (b) Analysis of promoter activities, based on LUC/REN ratios, in *Nicotiana benthamiana* leaves co-expressing PtrABF2, with or without PtrSnRK2.4, and the ADC promoter containing wild-type or mutated ABRE element. LUC/REN ratio of the negative control (SK+ 0800-pADC) was set to 1 for normalization. (c) Representative LUC bioluminescence in the leaf sections infiltrated with the designated constructs. (d) Promoter activities, based on LUC/REN ratios, in *N. benthamiana* leaves co-expressing PtrABF2 or PtrABF2^{S93A} with *PtrADC* promoter. (e) LUC bioluminescence image of *N. benthamiana* leaf sections expressing the designated constructs. (f, g) Expression level of *PtrADC* (f) and ADC activity (g) in callus transiently overexpressing PtrABF2-GFP or PtrABF2^{S93A}-GFP. (h) ADC activity in *N. benthamiana* leaves transiently co-expressing PtrABF2-GFP or PtrABF2^{S93A}-GFP, with or without HA-PtrSnRK2.4. (i) EMSA assays for examining the binding ability of PtrABF2 and PtrABF2^{S93A}, with or without His-PtrSnRK2.4, to the *PtrADC* promoter. The red and black triangles indicate bound and free probes, respectively. + and -, presence and absence of the components. Data in (b, d, f, g, h) are shown as means ± SE (n = 3). Asterisks indicate significant difference between the

indicated samples (**P < 0.01, ***P < 0.001), based on a one-way Fisher's least significant difference test.

Fig. 9. PtrSnRK2.4 functions positively in drought tolerance in transgenic lemon plants.

(a) Phenotype of transgenic (#2, #6) and wild type (WT) lemon plants before and after the drought treatment deprivation of watering for 25 d, then rewatered and grew for another 3 d). Scale bars = 2 cm. (b-h) Electrolyte leakage (b), MDA content (c), chlorophyll fluorescence (d), Fv/Fm ratios (e) and *in situ* accumulation of H_2O_2 and $O_2^{\cdot-}$ (f), ADC activity (g) and putrescine content (h) in the tested lines before and after the drought treatment. FW, fresh weight. Data in (b, c, e, g, h) are shown as means ± SE (n = 3). Asterisks indicate significant difference between transgenic lines and WT under drought stress (**P < 0.01, ***P < 0.001), based on a one-way Fisher's least significant difference test.

Fig. 10. Knockdown of *PtrSnRK2.4* leads to enhanced drought susceptibility by impairing putrescine accumulation.

(a-h) Plant phenotype (a), electrolyte leakage (b), MDA content (c), chlorophyll fluorescence imaging (d), Fv/Fm ratios (e), *in situ* accumulation of H_2O_2 and $O_2^{\cdot-}$ (f) and putrescine content (g) of VIGS line (TRV-PtrSnRK2.4), with or without putrescine pretreatment, and TRV control (TRV) before and after the drought treatment. Scale bars = 2 cm. FW, fresh weight. Data in (b, c, e, g) are shown as means ± SE (n = 3). Asterisks indicate significant difference between the indicated samples under the same growth conditions (**P < 0.01, ***P < 0.001), based on a one-way Fisher's least significant difference test.

Fig. 11. A working model illustrating the regulatory role of the molecular module SnRK2.4-ABF2-*ADC* in putrescine accumulation under drought stress. Drought stress leads to synthesis of ABA and triggers the ABA signaling, leading to activation of PtrSnRK2.4. PtrSnRK2.4 interacts with and phosphorylates PtrABF2, which in turn transcriptionally activates *PtrADC*, promoting putrescine biosynthesis and accumulation

for enhanced drought tolerance.

Supporting Information

Fig. S1. A phylogenetic tree constructed based on PtrABF2 and bZIP proteins of *Arabidopsis thaliana*.

Fig. S2. Analysis of GFP protein level in the callus transiently expressing *PtrABF2-GFP* by western blotting using an anti-GFP antibody.

Fig. S3. Expression patterns of *PtrABF1, PtrABF3, PtrABF4* in response to dehydration and abscisic acid (ABA) treatment.

Fig. S4. Expression patterns of *PtrABF2* in response to NaCl and cold treatment.

Fig. S5. Molecular identification of transgenic lemon plants overexpressing *PtrABF2*.

Fig. S6. Expression levels of *PtrABF2* and *PtrADC* in the TRV-PtrABF2 plants.

Fig. S7. Expression levels of *PtrABFs* in the TRV-PtrABF2 plants.

Fig. S8. The chlorophyll fluorescence and ROS levels in the TRV-PtrABF2 line.

Fig. S9. Phylogenetic analysis of SnRK2 proteins from different species.

Fig. S10. Relative expression of *PtrSnRK2s* at the designated time points under different treatments.

Fig. S11. Subcellular localization of PtrSnRK2.4.

Fig. S12. Analysis of the phosphorylation sites of PtrABF2 by PtrSnRK2.4 based on LC-MS/MS.

Fig. S13. Analysis of GFP protein levels in the callus transiently expressing *PtrABF2-GFP* and *PtrABF2^{S93A}-GFP* by western blotting using an anti-GFP antibody.

Fig. S14. PtrSnRK2.4-mediated phosphorylation of PtrABF2 increases putrescine content.

Fig. S15. Generation and molecular identification of transgenic lemon overexpressing *PtrSnRK2.4*.

Fig. S16. Expression analysis of related genes in the TRV-PtrSnRK2.4 VIGS plants.

Fig. S17. Expression level of two *PtrSnRK2* genes in TRV control and TRV2-PtrSnRK2.4 plants.

Table S1. List of primers used in this study.

Table S2. Accession numbers or locus IDs of the genes used for construction of the phylogenetic tree.

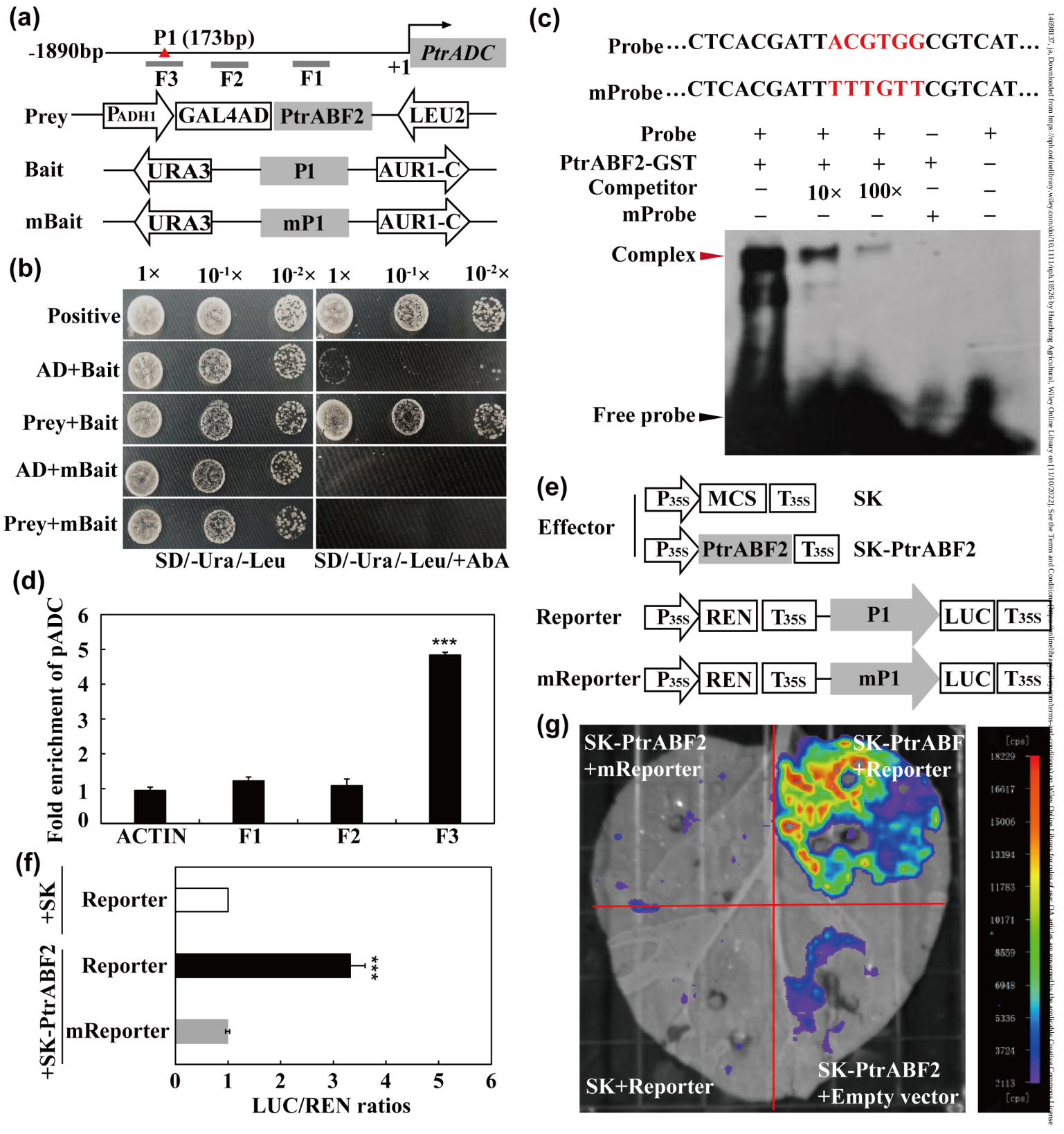

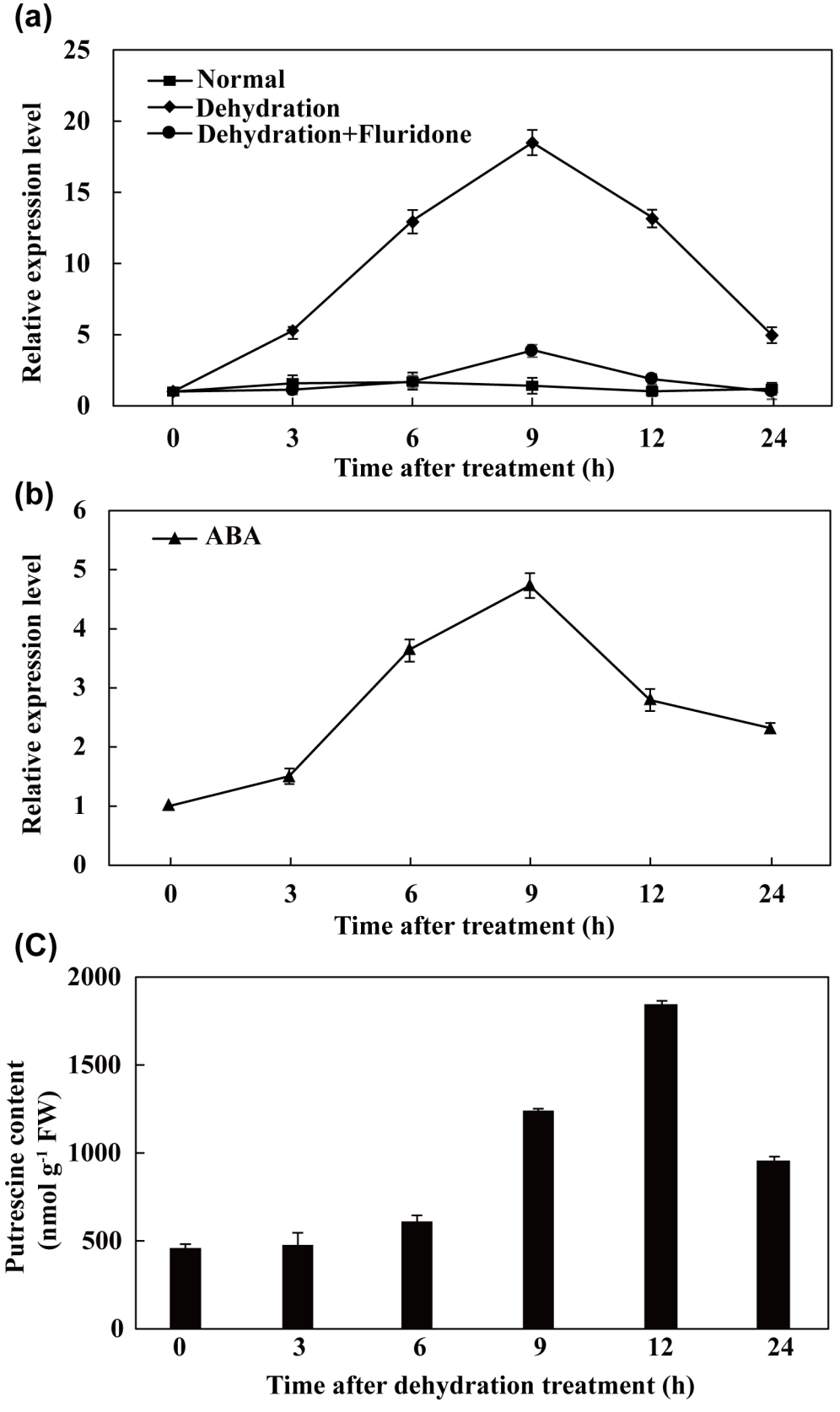

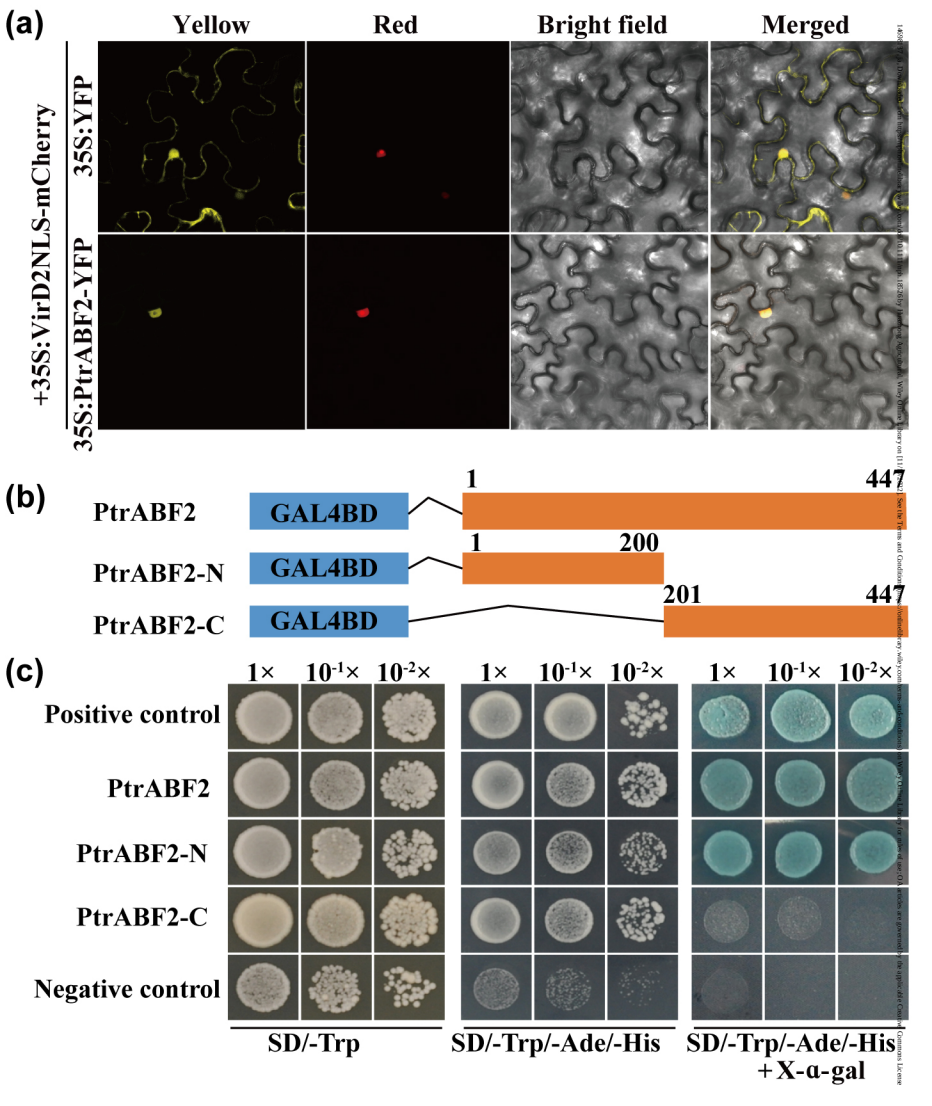
(a)
Yellow
Red
Bright field
Merged
+35S:VirD2NLS-mCherry
35S:YFP
35S:PtrABF2-YFP
(b)
PtrABF2
GAL4BD
1
447
PtrABF2-N
GAL4BD
1
200
PtrABF2-C
GAL4BD
201
447
(c)
1×
10-1×
10-2×
Positive control
PtrABF2
PtrABF2-N
PtrABF2-C
Negative control
SD/-Trp
SD/-Trp/-Ade/-His
SD/-Trp/-Ade/-His
+X-α-gal

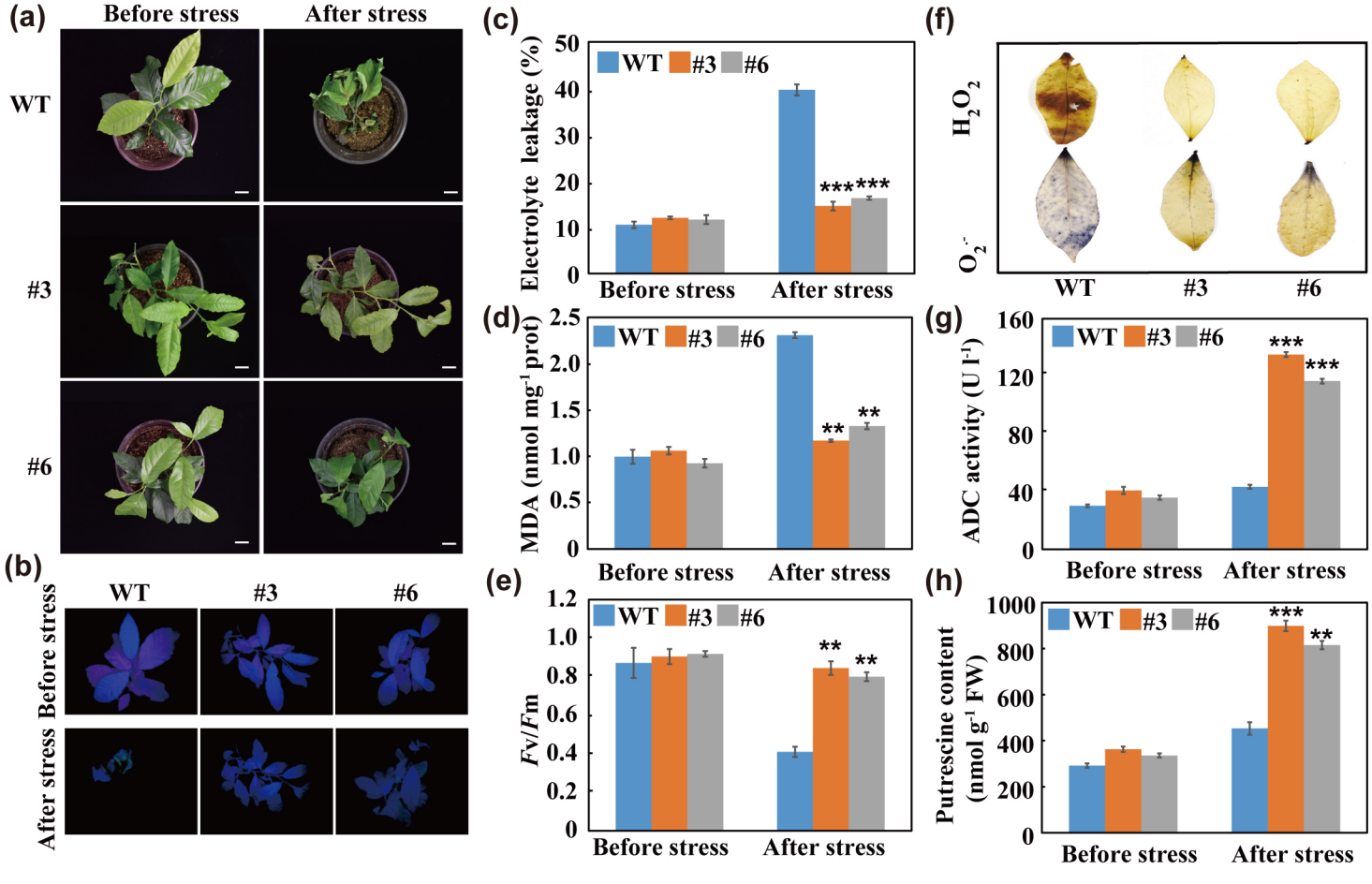
(a)
Before stress
After stress
WT
#3
#6
(b)
WT
#3
#6
Before stress
After stress
(c)
Electrolyte leakage (%)
WT #3 #6
***
***
Before stress
After stress
(d)
MDA (nmol mg-1 prot)
WT #3 #6
**
**
Before stress
After stress
(e)
Fv/Fm
WT #3 #6
**
**
Before stress
After stress
(f)
H2O2
O2·-
WT
#3
#6
(g)
ADC activity (U l-1)
WT #3 #6
***
***
Before stress
After stress
(h)
Putrescine content (nmol g-1 FW)
WT #3 #6
***
**
Before stress
After stress

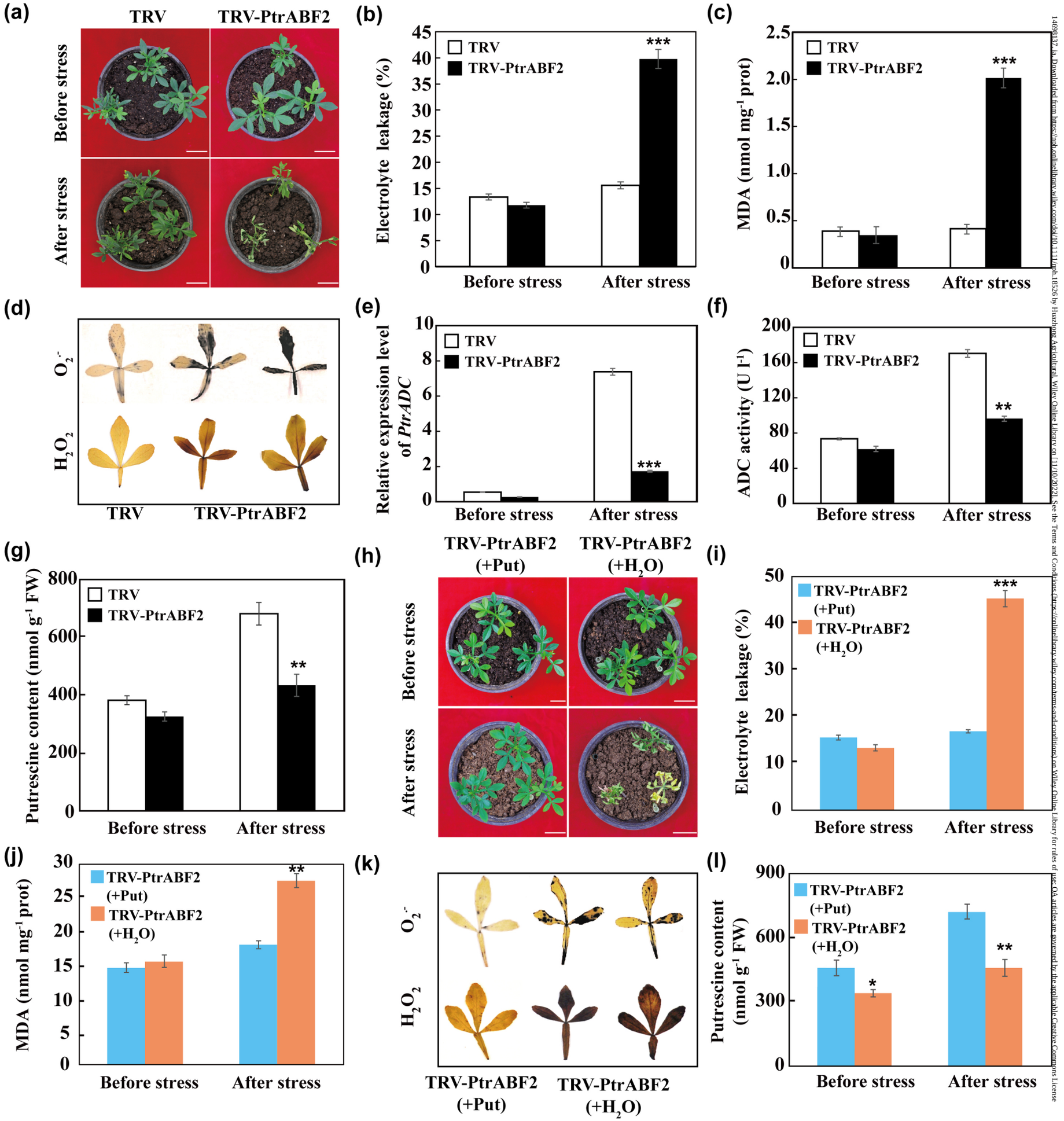

(a)

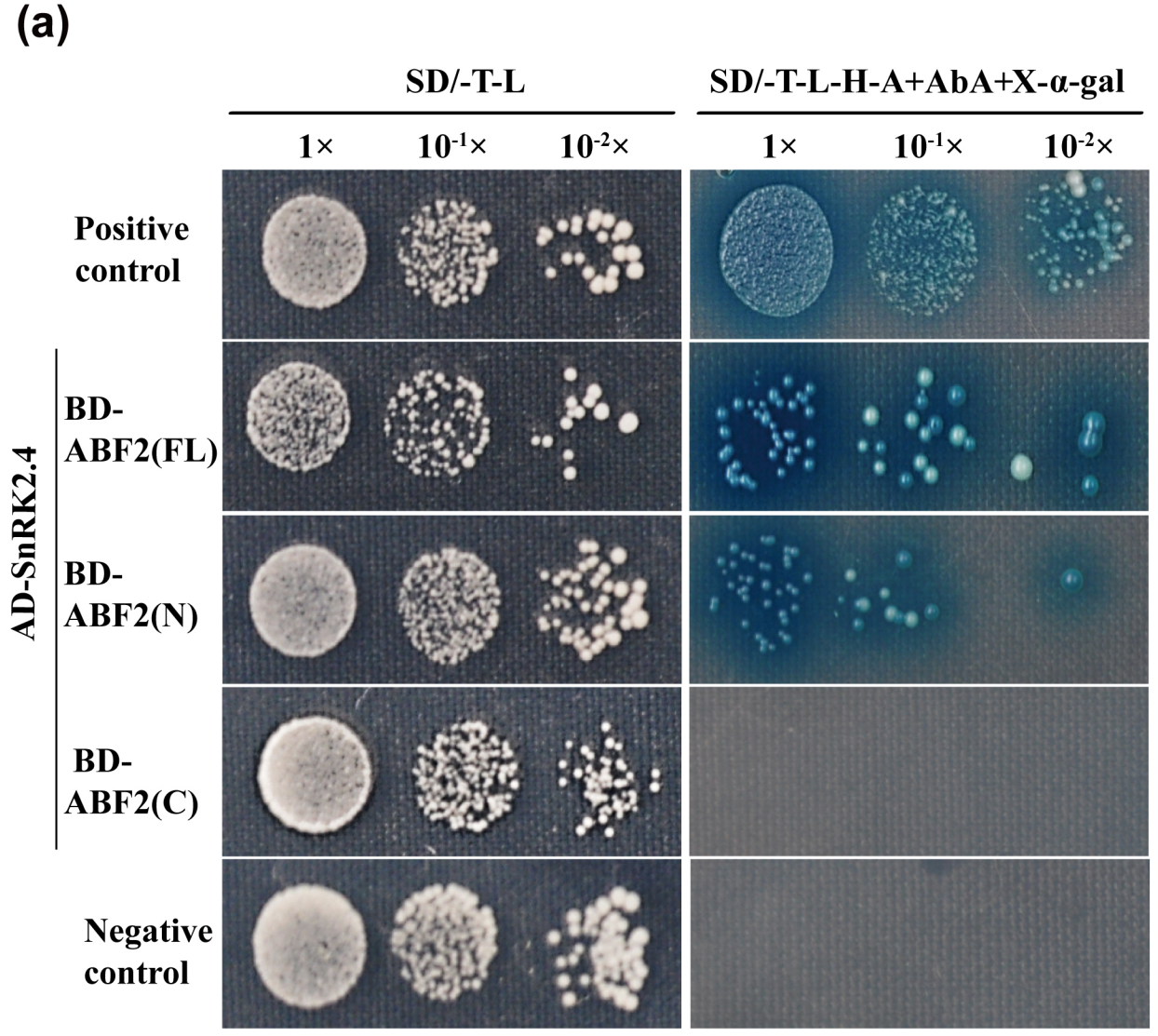

(b)

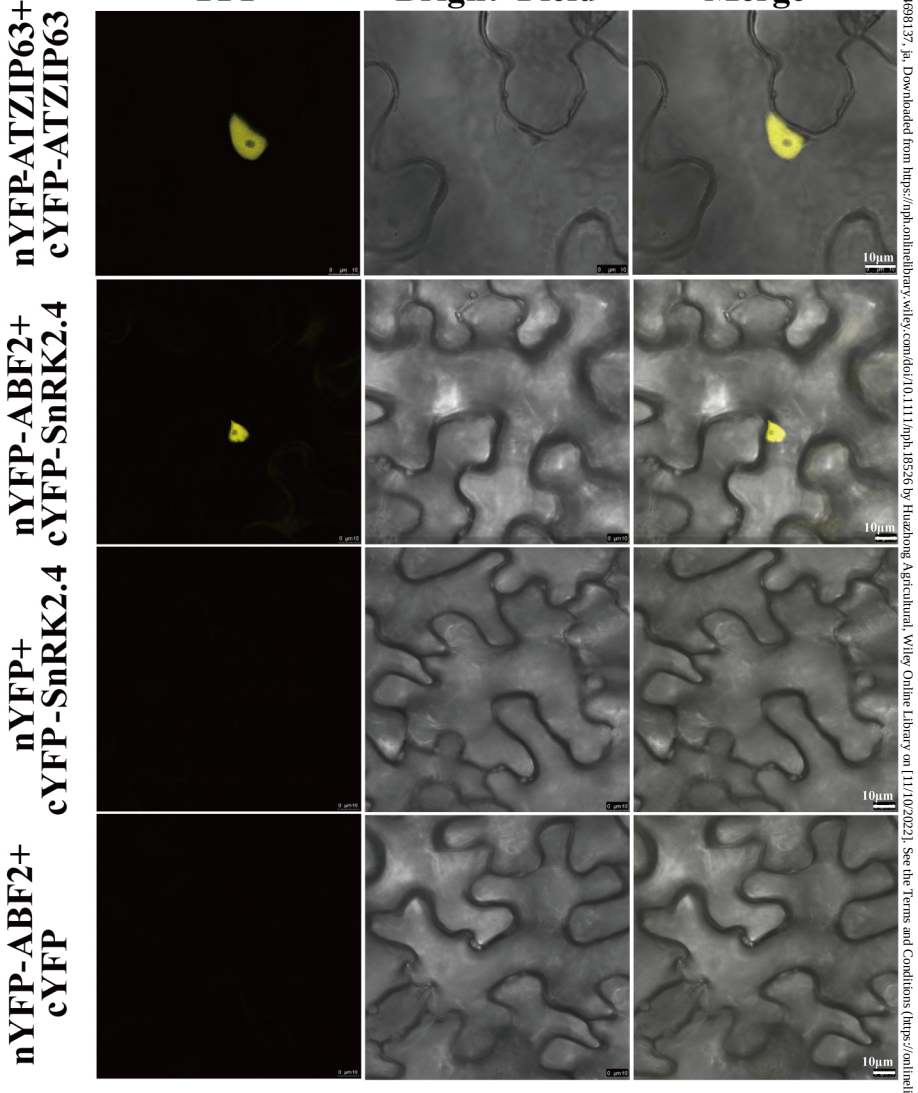

(c)

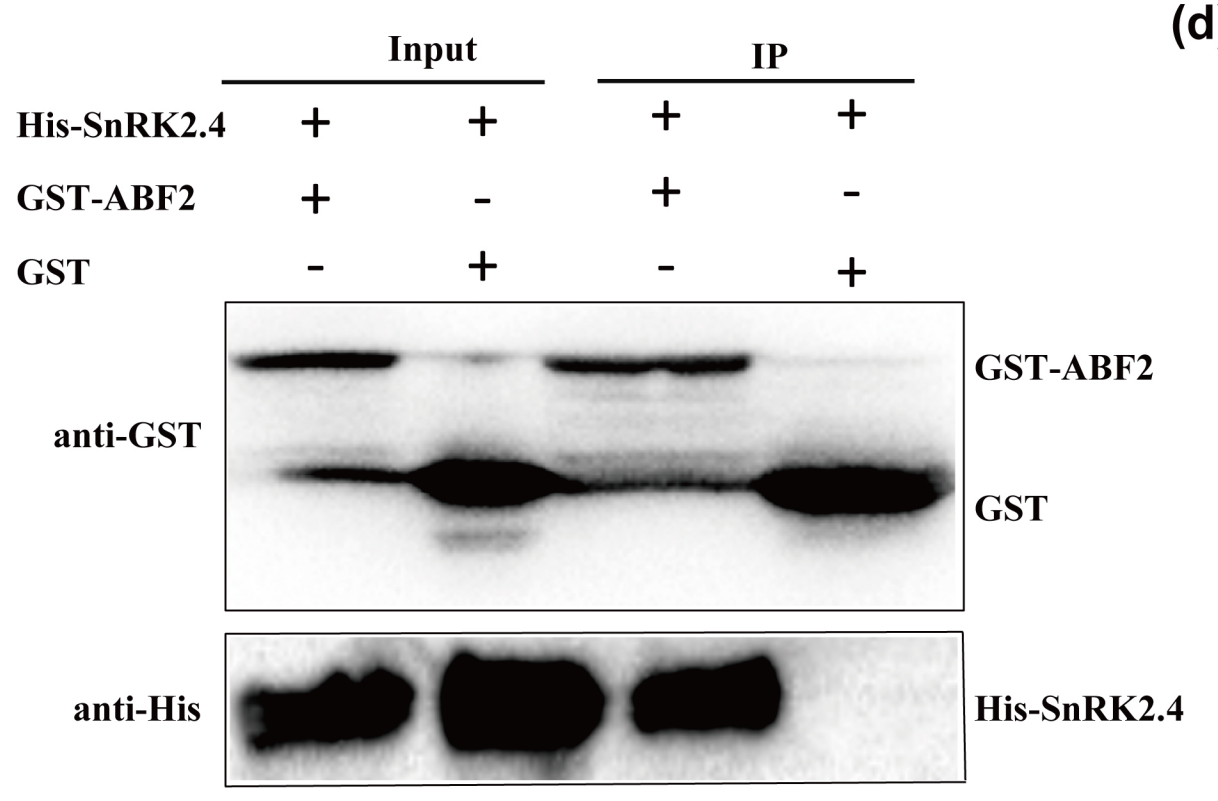

(d)

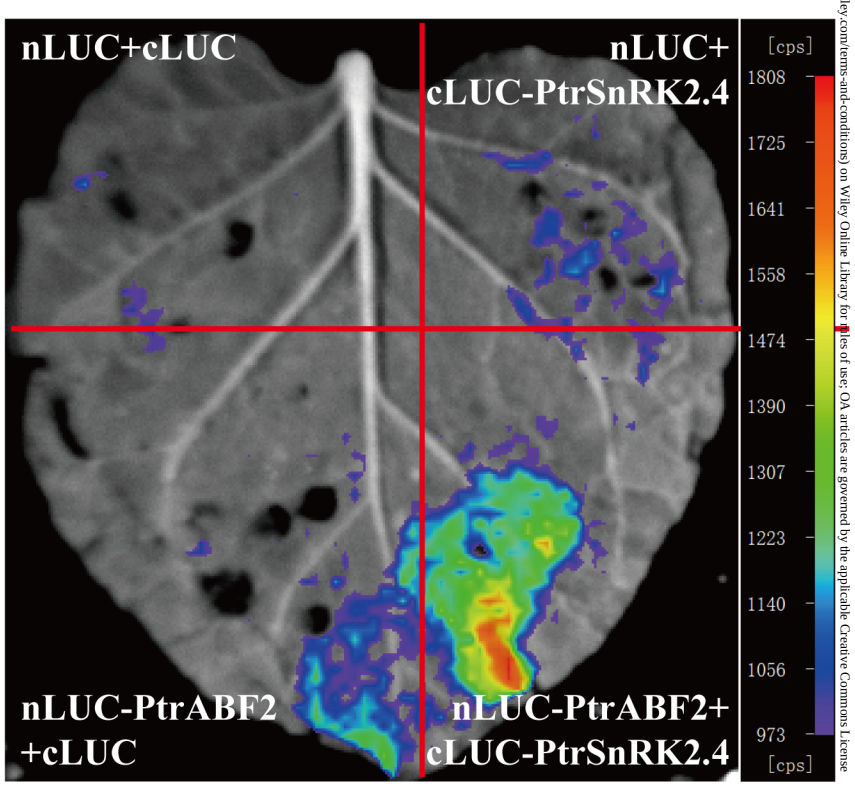

(a)

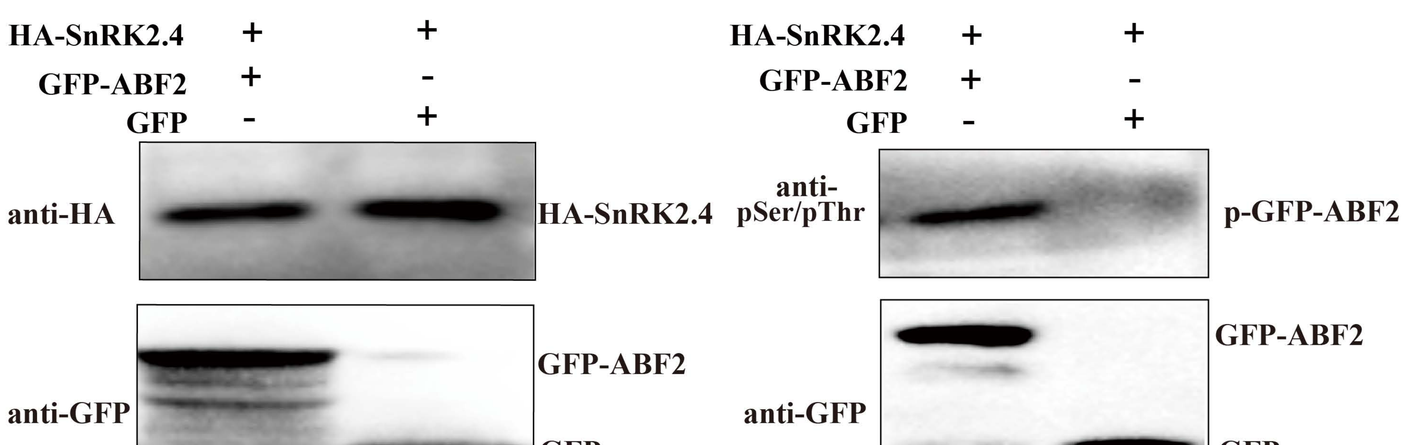

(b)

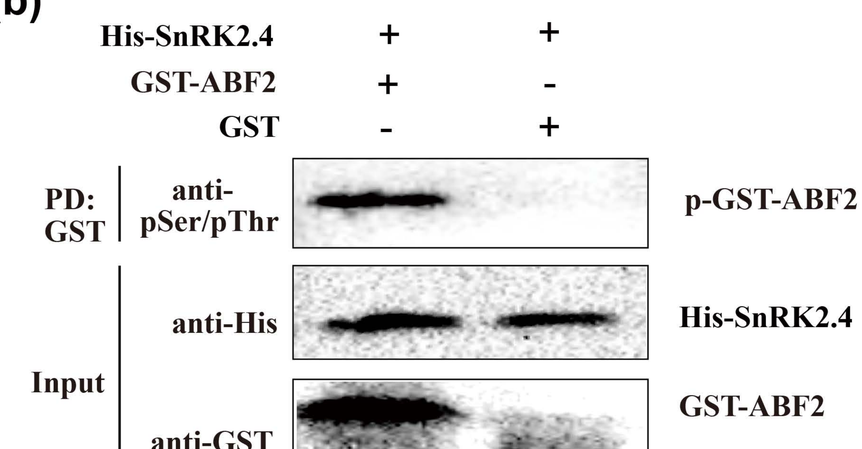

(c)

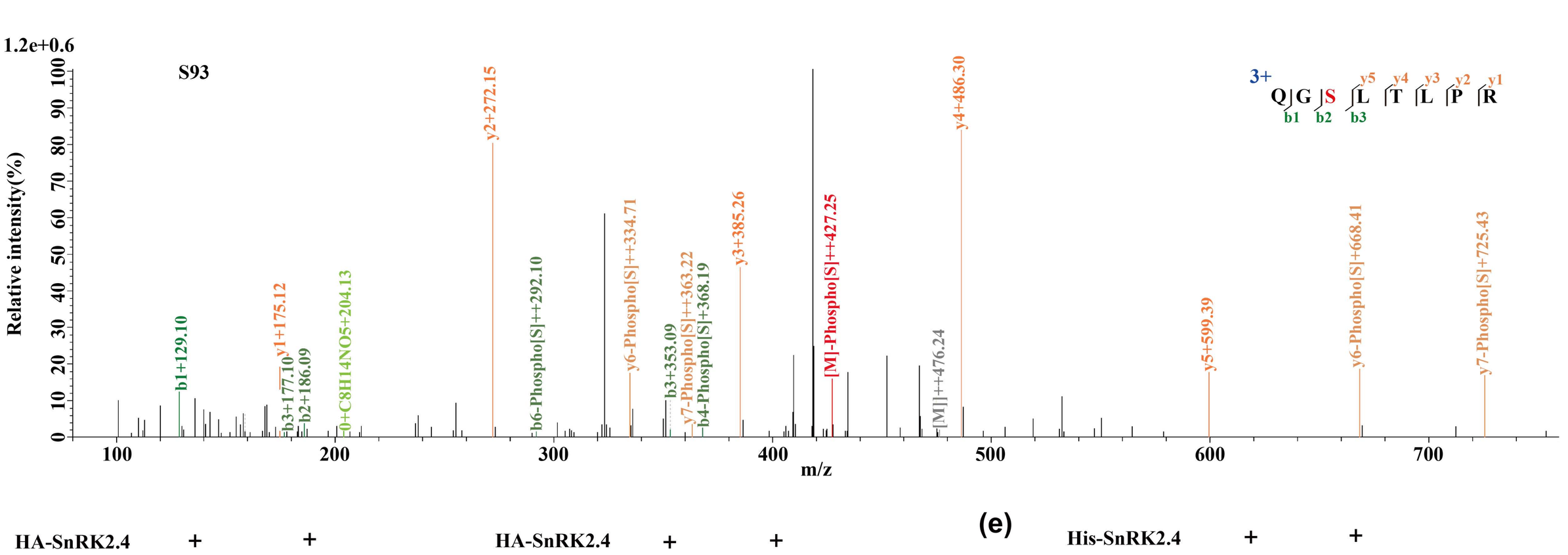

(d)

(e)

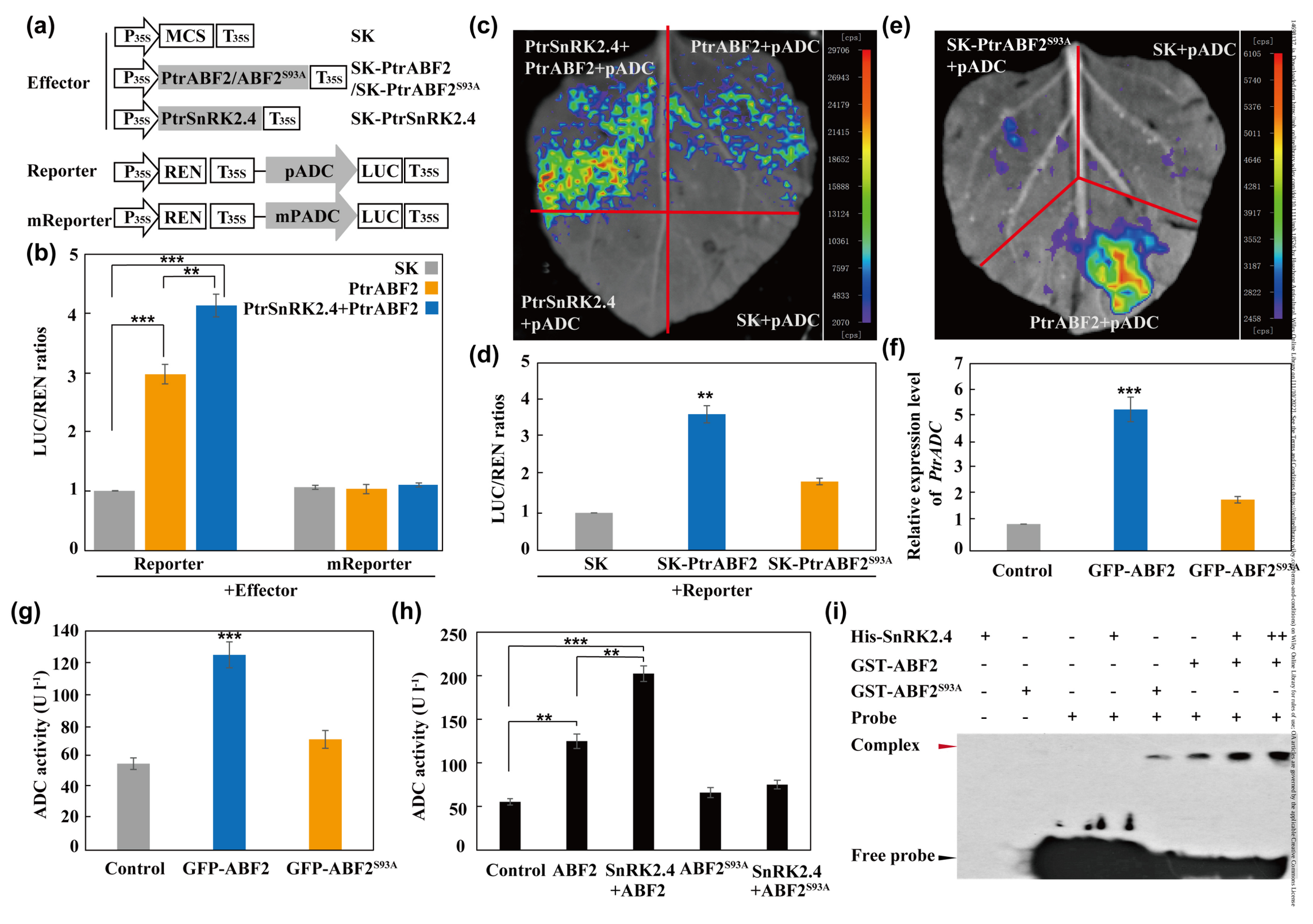
(a)
Effector
P35S
MCS
T35S
SK
PtrABF2/ABF2S93A
SK-PtrABF2
/SK-PtrABF2S93A
PtrSnRK2.4
SK-PtrSnRK2.4
Reporter
REN
pADC
LUC
mReporter
mPADC
(b)
LUC/REN ratios
SK
PtrABF2
PtrSnRK2.4+PtrABF2
Reporter
mReporter
+Effector
(c)
PtrSnRK2.4+
PtrABF2+pADC
PtrABF2+pADC
PtrSnRK2.4
+pADC
SK+pADC
[cps]
(d)
LUC/REN ratios
SK
SK-PtrABF2
SK-PtrABF2S93A
+Reporter
(e)
SK-PtrABF2S93A
+pADC
SK+pADC
PtrABF2+pADC
(f)
Relative expression level
of PtrADC
Control
GFP-ABF2
GFP-ABF2S93A
(g)
ADC activity (U l-1)
Control
GFP-ABF2
GFP-ABF2S93A
(h)
ADC activity (U l-1)
Control
ABF2
SnRK2.4
+ABF2
ABF2S93A
SnRK2.4
+ABF2S93A
(i)
His-SnRK2.4
GST-ABF2
GST-ABF2S93A
Probe
Complex
Free probe